

Spectroscopy and production of doubly charmed tetraquarks

Tetsuo Hyodo^a, Yan-Rui Liu^b, Makoto Oka^{c,d}, Shigehiro Yasui^c

^a*Yukawa Institute for Theoretical Physics, Kyoto University, Kyoto 606-8502, Japan*

^b*School of Physics, Shandong University, Jinan, 250100, P. R. China*

^c*Department of Physics, Tokyo Institute of Technology, Tokyo 152-8551, Japan*

^d*Advanced Science Research Center, Japan Atomic Energy Agency, Tokai, Ibaraki, 319-1195, Japan*

Abstract

We discuss the production of the exotic doubly-charmed tetraquark mesons $T_{cc}(cc\bar{u}\bar{d})$ from electron-positron collisions. $T_{cc}(cc\bar{u}\bar{d})$ is a compact exotic hadron whose binding energy is provided by the diquark correlations. We evaluate the production cross section in the electron-positron collisions using the nonrelativistic QCD framework, and investigate the difference of the production cross section for different color configurations in two charm quarks (antitriplet and sextet), where the mixing of different configurations is suppressed in the heavy quark limit. The total cross section is estimated by modeling the nonperturbative fragmentation process of the charm quark pair into the tetraquark by the wavefunction of the tetraquark and the probability of picking up the light quarks. We find that the internal color configurations are distinguishable by the qualitative features of the differential cross sections which are independent of the nonperturbative matrix elements.

Keywords: exotic tetraquark mesons, NRQCD, e^+e^- collisions, heavy quark

1. Introduction

Recent developments of the high energy experiments (Belle, Babar, BE-SIII, LHCb, *etc.*) have shown the existence of many exotic configuration of

Email addresses: hyodo@yukata.kyoto-u.ac.jp (Tetsuo Hyodo), yasuis@th.phys.titech.ac.jp (Shigehiro Yasui)

hadrons in the heavy quark sector [1–10]. To explain the nonconventional properties of the exotic hadrons, various internal structures have been proposed, such as multiquarks, hadronic molecules, gluon hybrids, and so on. Although there is no fundamental principle to forbid the exotic states in QCD, experimentally observed spectrum of hadrons is almost occupied by the conventional configurations [11]. To understand the rich nonperturbative dynamics of the strong interaction in the heavy hadron spectroscopy, it is important to study how the exotic hadrons are formed and how they are possibly produced in experiments.

There is a candidate of manifestly exotic hadrons in the heavy sector, the tetraquark T_{cc} state which contains two charm quarks and two light antiquarks ($cc\bar{u}\bar{d}$). The isospin and spin-parity quantum numbers are considered to be $I(J^P) = 0(1^+)$, based on the color-magnetic interaction. Because of the spin-parity, the lowest energy two-meson channel to which T_{cc} can couple is the s -wave DD^* pair. Because it requires at least four valence quarks, T_{cc} is classified as the manifestly exotic hadrons, which contain the pentaquark $\Theta^+(uudd\bar{s})$ [12, 13]. Now, several manifestly exotic hadrons with heavy flavor have been observed, e.g., the charged charmonium-like states $Z_c(c\bar{c}u\bar{d})$ [14, 15] and bottomonium-like states $Z_b(b\bar{b}u\bar{d})$ [16] (see the reviews [2, 5] for more information) as well as the new candidate of pentaquark $P_c(c\bar{c}uud)$ recently reported by LHCb [17]. The existence of T_{cc} is theoretically predicted and this tetraquark is still a promising state to be found. The T_{cc} state was originally proposed in the context of the constituent quark models [18, 19] (see also Ref. [20]). The investigation is further pursued in quark models [21–29], including dynamical four-body calculations [30–37]. The role of the strong diquark correlation is emphasized in Refs. [38–40]. Another approach is based on the hadronic molecule picture, by constructing the potential between D and D^* [41–46]. The DD^* potential is recently studied in lattice QCD [47], and was found to be attractive. The properties of T_{cc} are also discussed in the context of the heavy quark symmetry argument [48] and of the QCD sum rules [49, 50].

One of the unique features of the multiquark hadrons is the color configurations. In ordinary mesons and baryons, the quark-quark (quark-antiquark) correlation is limited in the color anti-triplet $\bar{\mathbf{3}}$ (singlet $\mathbf{1}$) representation. The color sextet $\mathbf{6}$ quark-quark correlation (color octet $\mathbf{8}$ quark-antiquark correlation) is only allowed in the totally color-singlet system with more than three quarks. Thus, the tetraquark is the simplest system in which we can investigate the exotic color correlations. In this paper, we first summarize

the spectroscopy of the T_{cc} states in the constituent quark model picture with different color configurations. We also discuss the spatial correlations of quarks inside T_{cc} with the quark model.

Another purpose of this paper is to study the production cross section for the orientation of experimental searches. So far, the production yield of heavy exotics including T_{cc} has been estimated for the heavy ion collisions [51–53]. Here we focus on the electron-positron collisions. The double charm production such as $e^+e^- \rightarrow J/\psi + (c\bar{c})$ with $(c\bar{c})$ being any states with a charm quark and a charm antiquark (inclusive process) has been already observed experimentally [54–57]. By recombining the charm quarks in the final state of this process, we obtain the production of the doubly charmed hadrons. In fact, Refs. [58–60] have theoretically discussed the production of doubly heavy baryon Ξ_{cc} , which is recently observed in proton-proton collisions by the LHCb collaboration [61]. The production of T_{cc} is thus naturally expected as a process $e^+e^- \rightarrow T_{cc} + (c\bar{c})$, in the same manner [62]. In Ref. [62], to estimate the production cross sections, we utilize the nonrelativistic QCD (NRQCD) framework [63, 64], which is an effective field theory of QCD with the velocity expansion and the factorization of the production processes. However, the number of the production of light quarks was not considered in the previous work [62], and hence we obtained the conclusion that the production cross section of T_{cc} is the same as that of Ξ_{cc} . This is clearly not realistic, because the production cross section of T_{cc} should be smaller than that of Ξ_{cc} due to the different number of light quarks. In the present work, we consider the factor of the light quark production and estimate the production cross section of T_{cc} in more realistic way.

The paper is organized as follows. In section 2, we discuss the mass spectrum of the T_{cc} states with various color/flavor configurations based on the diquark picture, and in section 3 we calculate the wave functions of T_{cc} in the constituent quark model. In section 4, we explain the NRQCD framework for the production of T_{cc} in the electron-positron collisions. In section 5, we present the numerical results of the production cross sections. The last section is devoted to the summary. Based on the analysis in the previous paper Ref. [62], we further discuss the decay mode of T_{cc} , the fragmentation process, and the energy and angular dependence of the cross sections, together with a detailed account of the formulation.

2. Spectrum and decay of tetraquark T_{cc}

2.1. Quark correlation and diquark picture

The mass of T_{cc} has been studied theoretically in quark models by many authors [18–40]. Their results can be essentially understood by the strong diquark correlation in the constituent quark picture [39, 40]. To appreciate this, we consider the interaction Hamiltonian through the color-spin interaction [65];

$$H_{\text{int}} = \sum_{i < j} \frac{C_H}{m_i m_j} \left(-\frac{3}{8} \right) \vec{\lambda}_i \cdot \vec{\lambda}_j \vec{s}_i \cdot \vec{s}_j. \quad (1)$$

where $\vec{\lambda}_i$ is the Gell-Mann matrix for color SU(3) acting on the quark i , and $\vec{s}_i = \vec{\sigma}_i/2$ is the spin operator with the Pauli matrix $\vec{\sigma}_i$ for the quark i . We introduce the factor $-3/8$ for the normalization of the pair of quarks in color antitriplet channel; $\langle \bar{\mathbf{3}} | (-3/8) \vec{\lambda}_i \cdot \vec{\lambda}_j | \bar{\mathbf{3}} \rangle = 1$. The matrix elements of the operator $(-3/8) \vec{\lambda}_i \cdot \vec{\lambda}_j \vec{s}_i \cdot \vec{s}_j$ for quark pairs in different color-spin channels are summarized in Table 1. The interaction is specified by the coupling strength C_H and the mass of the quark m_i . In principle, the coupling strength C_H reflects the spatial correlation of the quark pair. For instance, with the delta function type interaction, C_H is proportional to $\langle \delta(r) \rangle$ with the relative distance of the quark pair r . The expectation value is dynamically determined by the wavefunction of each hadron. Here we take a simpler approach [39, 40] where C_H is taken to be a constant and adjusted to reproduce the mass splittings of known hadrons. Fixing the quark masses as $m_u = m_d = 300$ MeV and $m_c = 1500$ MeV, we determine the constant $C_H = C_{qq}$ for the quark-quark pair by the mass splitting of baryons, $M_\Delta - M_N$, $M_\Sigma - M_\Lambda$, $M_{\Sigma_c} - M_{\Lambda_c}$, and $M_{\Sigma_b} - M_{\Lambda_b}$. In the same way, the constant $C_H = C_{q\bar{q}}$ for the quark-antiquark pair is determined by $M_\rho - M_\pi$, $M_{K^*} - M_K$, $M_{D^*} - M_D$, and $M_{B^*} - M_B$. We obtain $C_{qq} = (193 \text{ MeV}) m_u^2$ and $C_{q\bar{q}} = (318 \text{ MeV}) m_u^2$ which reproduce well the observed mass splittings [40].

In the above determination of C_{qq} and $C_{q\bar{q}}$, the correlation between two charm quarks is not considered. The coupling strength C_H for heavy-heavy (cc) quark pair should be modified from those of light-light and heavy-light quark pairs, when the spatial structure is taken into account. Because the kinetic energy is suppressed in the heavy system, the wave function of the heavy-heavy quark pair is spatially shrunk so that the expectation value $\langle \delta(r) \rangle$ increases. This effectively enhances the coupling strength. In fact,

Table 1: The matrix elements of the operator $(-3/8)\vec{\lambda}_i \cdot \vec{\lambda}_j \vec{s}_i \cdot \vec{s}_j$ for quark pairs in spin $s = 0, 1$ and color $\bar{\mathbf{3}}, \mathbf{6}, \mathbf{1}, \mathbf{8}$ configurations.

	$\bar{\mathbf{3}}$	$\mathbf{6}$	$\mathbf{1}$	$\mathbf{8}$
$s = 0$	$-3/4$	$3/8$	$-3/2$	$3/16$
$s = 1$	$1/4$	$-1/8$	$1/2$	$-1/16$

the mass splitting of charmonia (J/ψ and η_c) leads to $C_{c\bar{c}} = (59 \text{ MeV})m_c^2 = (1475 \text{ MeV})m_u^2$ which is much larger than C_{qq} . Because $C_{qq}/C_{q\bar{q}} \sim 2/3$, we determine $C_{cc} = 2C_{c\bar{c}}/3 = (39 \text{ MeV})m_c^2 = (975 \text{ MeV})m_u^2$. In practice, the enhancement of the coupling strength in the charm sector does not cause major difference [39, 40], because the heavy-heavy interaction is in any case suppressed by $1/m_c^2$ factor.

Many properties of hadron masses are well understood by the diquark picture. To focus on the inter-quark correlations, we regard a pair of quarks as one single cluster called diquark [66].¹ We define the mass of the diquark by the sum of the quark masses and the interaction energy. The latter is calculated from Eq. (1). For example, the ud diquark in Λ_c is combined into color $\bar{\mathbf{3}}$, spin 1S_0 in isospin $I = 0$. Because of the attractive quark-quark interaction, the mass of this diquark (so-called “good” diquark) is about 145 MeV below $2m_u$ [39, 40].² On the other hand, the mass of the ud diquark contained in Σ_c and Σ_c^* , with color $\bar{\mathbf{3}}$, but spin 3S_1 in isospin $I = 1$ (so-called “bad” diquark), is about 48 MeV above $2m_u$ due to the inter-quark repulsion. Thus we confirm that the mass splitting of several hadrons are well reproduced in the diquark picture. This indicates that the diquark picture can be used as a good estimation of the masses of exotic heavy hadrons also.

2.2. Mass spectrum of T_{cc} in diquark picture

We now turn to the study of mass of the exotic tetraquark T_{cc} in the diquark picture. The quark content of T_{cc} is $cc\bar{u}\bar{d}$, which is described by

¹We note that the diquark is not necessarily a spatially compact object; the important fact is that there is a correlation of the specific quark pair.

²The attraction in this channel is a source to form a quark-quark pairing (Cooper pairing) in the color superconductivity in quark matter at high density [67–69].

the system of cc diquark plus $\bar{u}\bar{d}$ diquark. We consider the s -wave state as the lowest energy configuration. From Table 1, the most attractive qq configuration is in color $\bar{\mathbf{3}}$ and spin 1S_0 . We thus consider the ground state of T_{cc} consists of a “good” $\bar{u}\bar{d}$ diquark with color $\mathbf{3}$ and spin 1S_0 . The antisymmetrization of the quarks leads to the isospin $I = 0$. To form the color singlet, the cc diquark should be combined into color $\bar{\mathbf{3}}$. Because there is no flavor degrees of freedom, the spin of the cc diquark should be 3S_1 . By combining two diquarks in relative s wave, the total quantum number of T_{cc} is given by $I(J^P) = 0(1^+)$. We note that the cc diquark induces a repulsive interaction, but this is suppressed by the $1/m_c^2$ factor in the interaction Hamiltonian H_{int} in Eq. (1). The dominant contribution of the color-spin interaction is the attraction in the $\bar{u}\bar{d}$ diquark.

To investigate the stability of T_{cc} in the diquark model, we compare its mass with the lowest two-meson threshold [39, 40]. For $I(J^P) = 0(1^+)$ channel, this is the DD^* threshold. The binding energy from the DD^* threshold is estimated as

$$\text{B.E.} = \left(-\frac{3}{2} \frac{C_{q\bar{q}}}{m_u m_c} + \frac{1}{2} \frac{C_{q\bar{q}}}{m_u m_c} \right) - \left(-\frac{3}{4} \frac{C_{qq}}{m_u^2} + \frac{1}{4} \frac{C_{cc}}{m_c^2} \right) \simeq 71 \text{ MeV}, \quad (2)$$

where the first term is the interaction energy of the color-spin interaction for $c\bar{q}$ pairs in the D and D^* mesons and the second term is that in T_{cc} . We note that the interaction energy of the heavy-light pairs are cancelled out in T_{cc} . Because the binding energy is positive, we find that this state is stable against the strong decay. The obtained binding energy is consistent with the results of the fully dynamical calculation in the constituent quark model [30–37] and that in the QCD sum rule [49].³

Thus the attraction in the $\bar{u}\bar{d}$ diquark in color $\mathbf{3}$, spin 1S_0 and isospin $I = 0$ is essential for the stable T_{cc} . In addition to this channel, however, there is also an attraction in another channel, color $\bar{\mathbf{6}}$, spin 3S_1 and isospin $I = 0$, in $\bar{u}\bar{d}$ diquark (see Table 1). This suggests the possibility to form a new state of T_{cc} with cc pair in color $\mathbf{6}$ and spin 1S_0 and $\bar{u}\bar{d}$ pair in color $\bar{\mathbf{6}}$ and spin 3S_1 . We note the color configurations of the quark pairs ($\mathbf{6}$ and $\bar{\mathbf{6}}$) are orthogonal to the conventional T_{cc} discussed above ($\bar{\mathbf{3}}$ and $\mathbf{3}$). Although the strength of the attraction is smaller (factor $-1/8$ in Table 1) than that

³We however note that the QCD sum rule analysis in Ref. [50] does not conclude the existence of stable doubly charmed tetraquarks.

of the $\bar{u}\bar{d}$ diquark in color $\mathbf{3}$ (factor $-3/4$), this new configuration can be a candidate of the first excited state of the conventional T_{cc} . In the following, we refer to the conventional (new) state as $T_{cc}[\mathbf{\bar{3}}, {}^3S_1]$ ($T_{cc}[\mathbf{6}, {}^1S_0]$) labeled by the quantum numbers of the cc pair. The color-spin configuration of quarks is summarized as follows:

$$|T_{cc}[\mathbf{\bar{3}}, {}^3S_1]\rangle \sim |[\bar{u}\bar{d}]_{\mathbf{3}, {}^1S_0, I=0}[cc]_{\mathbf{\bar{3}}, {}^3S_1}\rangle, \quad (3)$$

$$|T_{cc}[\mathbf{6}, {}^1S_0]\rangle \sim |[\bar{u}\bar{d}]_{\mathbf{\bar{6}}, {}^3S_1, I=0}[cc]_{\mathbf{6}, {}^1S_0}\rangle. \quad (4)$$

For later convenience, we present the recombination factor in color space

$$|[\bar{u}\bar{d}]_{\mathbf{3}}[c_1c_2]_{\mathbf{\bar{3}}}\rangle = \frac{1}{\sqrt{3}}|[\bar{u}c_1]_{\mathbf{1}}[\bar{d}c_2]_{\mathbf{1}}\rangle - \sqrt{\frac{2}{3}}|[\bar{u}c_1]_{\mathbf{8}}[\bar{d}c_2]_{\mathbf{8}}\rangle \quad (5)$$

$$= -\frac{1}{\sqrt{3}}|[\bar{u}c_2]_{\mathbf{1}}[\bar{d}c_1]_{\mathbf{1}}\rangle + \sqrt{\frac{2}{3}}|[\bar{u}c_2]_{\mathbf{8}}[\bar{d}c_1]_{\mathbf{8}}\rangle. \quad (6)$$

This suggests that the fraction of color singlet (octet) $\bar{q}q$ pairs is $1/3$ ($2/3$). The wavefunction of $T_{cc}[\mathbf{6}, {}^1S_0]$ can also be rearranged as

$$|[\bar{u}\bar{d}]_{\mathbf{\bar{6}}}[c_1c_2]_{\mathbf{6}}\rangle = \sqrt{\frac{2}{3}}|[\bar{u}c_1]_{\mathbf{1}}[\bar{d}c_2]_{\mathbf{1}}\rangle + \frac{1}{\sqrt{3}}|[\bar{u}c_1]_{\mathbf{8}}[\bar{d}c_2]_{\mathbf{8}}\rangle \quad (7)$$

$$= \sqrt{\frac{2}{3}}|[\bar{u}c_2]_{\mathbf{1}}[\bar{d}c_1]_{\mathbf{1}}\rangle + \frac{1}{\sqrt{3}}|[\bar{u}c_2]_{\mathbf{8}}[\bar{d}c_1]_{\mathbf{8}}\rangle. \quad (8)$$

Because the total quantum number of $T_{cc}[\mathbf{6}, {}^1S_0]$ is $I(J^P) = 0(1^+)$, which is the same with $T_{cc}[\mathbf{\bar{3}}, {}^3S_1]$, one may wonder that $T_{cc}[\mathbf{6}, {}^1S_0]$ can strongly mix with $T_{cc}[\mathbf{\bar{3}}, {}^3S_1]$, for instance, through the one gluon exchange. The transition process however needs to flip the spin of the heavy quark, because of the different spin configuration of the cc pair in $T_{cc}[\mathbf{6}, {}^1S_0]$ from that in $T_{cc}[\mathbf{\bar{3}}, {}^3S_1]$. Since the spin-flip amplitude is suppressed by $1/m_c$, the mixing probability of $T_{cc}[\mathbf{\bar{3}}, {}^3S_1]$ and $T_{cc}[\mathbf{6}, {}^1S_0]$ should be of the order of $1/m_c^2$. In the heavy quark limit, this mixing must vanish, while the splitting between $T_{cc}[\mathbf{\bar{3}}, {}^3S_1]$ and $T_{cc}[\mathbf{6}, {}^1S_0]$ remains as it comes from the mass difference of light diquarks (See Eq. (9) below). In a fully dynamical four-body quark-model calculation [36], the ground state of T_{cc} is almost dominated ($\sim 88\%$) by the component with the cc pair in color $\mathbf{\bar{3}}$. It is therefore a good approximation to neglect the mixing effect. It should be emphasized that the suppression of the mixing is ensured by the spin structure of the heavy diquark regardless to any model settings.

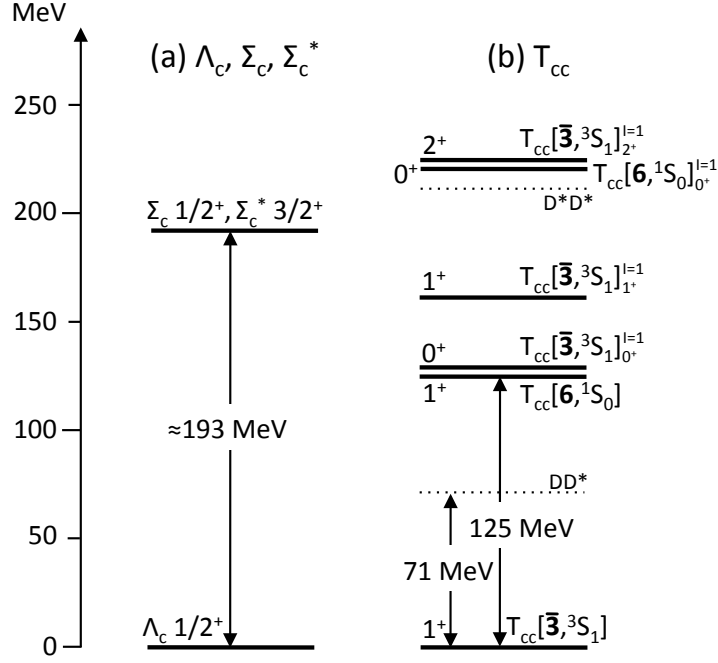


Figure 1: Mass spectra of (a) Λ_c , Σ_c and Σ_c^* baryons and of (b) T_{cc} . The quantum numbers of two charm quarks (cc) and two light antiquarks ($\bar{q}\bar{q}$) are shown.

Based on the suppression of the mixing, we estimate the mass splitting between $T_{cc}[\bar{\mathbf{3}}, {}^3S_1]$ and $T_{cc}[\mathbf{6}, {}^1S_0]$ by the color-spin interaction (1) as

$$M(T_{cc}[\mathbf{6}, {}^1S_0]) - M(T_{cc}[\bar{\mathbf{3}}, {}^3S_1]) = \left(-\frac{1}{8} \frac{C_{qq}}{m_u^2} + \frac{3}{8} \frac{C_{cc}}{m_c^2} \right) - \left(-\frac{3}{4} \frac{C_{qq}}{m_u^2} + \frac{1}{4} \frac{C_{cc}}{m_c^2} \right) \simeq 125 \text{ MeV}. \quad (9)$$

Thus, the mass of $T_{cc}[\mathbf{6}, {}^1S_0]$ is larger than that of $T_{cc}[\bar{\mathbf{3}}, {}^3S_1]$ by 125 MeV. In the heavy quark limit, $M(T_{cc}[\mathbf{6}, {}^1S_0]) - M(T_{cc}[\bar{\mathbf{3}}, {}^3S_1]) \rightarrow (5/8)C_{qq}/m_u^2 \simeq 121 \text{ MeV}$.

Next we consider the stability of $T_{cc}[\mathbf{6}, {}^1S_0]$ via the strong interaction.⁴ From the isospin conservation, the transition from $T_{cc}[\mathbf{6}, {}^1S_0]$ into $T_{cc}[\bar{\mathbf{3}}, {}^3S_1]$ should emit at least two pions. This is kinematically forbidden by the mass

⁴Possible weak and radiative decays will be discussed in section 2.3.

difference in Eq. (9). Combining the binding energy of $T_{cc}[\bar{\mathbf{3}}, {}^3S_1]$ (2) and the mass splitting (9), we find that $T_{cc}[\mathbf{6}, {}^1S_0]$ is located by 54 MeV above the DD^* threshold (see Fig. 1). Thus, $T_{cc}[\mathbf{6}, {}^1S_0]$ decays into D and D^* through the fall-apart process in s wave, and hence that the decay width of $T_{cc}[\mathbf{6}, {}^1S_0]$ may not be negligibly small. However, the color recombination in the process $[\bar{u}\bar{d}]_{\bar{\mathbf{6}}}[\text{cc}]_{\mathbf{6}} \rightarrow [\bar{u}c]_1[\bar{d}c]_1$ can suppress the decay width of $T_{cc}[\mathbf{6}, {}^1S_0]$.

Let us investigate the other possible excited states with higher masses for T_{cc} . For example, we may consider the $I = 1$ ud diquarks in $cc\bar{u}\bar{d}$. This combination leads to T_{cc} with $I(J^P) = 1(0^+)$, $1(1^+)$, and $1(2^+)$. Those states are denoted by $T_{cc}[\bar{\mathbf{3}}, {}^3S_1]_{0^+, 1^+, 2^+}^{I=1}$ and $T_{cc}[\mathbf{6}, {}^1S_0]_{0^+}^{I=1}$. Unlike the $I = 0$ case where no correlation between the heavy quark and the light antiquark exists, now the heavy-light correlation does not vanish. One may calculate its contributions in color and spin spaces separately and then combine the results together. Similar to Eqs. (5) and (6), we may get the recombination factor in spin space

$$\begin{aligned} |[\bar{u}\bar{d}]_{s=1}[c_1c_2]_{s=1}\rangle_{J=0} &= \frac{\sqrt{3}}{2}|[\bar{u}c_1]_{s=0}[\bar{d}c_2]_{s=0}\rangle_{J=0} - \frac{1}{2}|[\bar{u}c_1]_{s=1}[\bar{d}c_2]_{s=1}\rangle_{J=0} \\ &= \frac{\sqrt{3}}{2}|[\bar{u}c_2]_{s=0}[\bar{d}c_1]_{s=0}\rangle_{J=0} - \frac{1}{2}|[\bar{u}c_2]_{s=1}[\bar{d}c_1]_{s=1}\rangle_{J=0}, \end{aligned} \quad (10)$$

$$\begin{aligned} |[\bar{u}\bar{d}]_{s=1}[c_1c_2]_{s=1}\rangle_{J=1} &= \frac{1}{\sqrt{2}}|[\bar{u}c_1]_{s=1}[\bar{d}c_2]_{s=0}\rangle_{J=1} + \frac{1}{\sqrt{2}}|[\bar{u}c_1]_{s=0}[\bar{d}c_2]_{s=1}\rangle_{J=1} \\ &= \frac{1}{\sqrt{2}}|[\bar{u}c_2]_{s=1}[\bar{d}c_1]_{s=0}\rangle_{J=1} + \frac{1}{\sqrt{2}}|[\bar{u}c_2]_{s=0}[\bar{d}c_1]_{s=1}\rangle_{J=1}, \end{aligned} \quad (11)$$

$$|[\bar{u}\bar{d}]_{s=1}[c_1c_2]_{s=1}\rangle_{J=2} = |[\bar{u}c_1]_{s=1}[\bar{d}c_2]_{s=1}\rangle_{J=2} = |[\bar{u}c_2]_{s=1}[\bar{d}c_1]_{s=1}\rangle_{J=2}; \quad (12)$$

$$\begin{aligned} |[\bar{u}\bar{d}]_{s=0}[c_1c_2]_{s=0}\rangle_{J=0} &= \frac{\sqrt{3}}{2}|[\bar{u}c_1]_{s=1}[\bar{d}c_2]_{s=1}\rangle_{J=0} + \frac{1}{2}|[\bar{u}c_1]_{s=0}[\bar{d}c_2]_{s=0}\rangle_{J=0} \\ &= -\frac{\sqrt{3}}{2}|[\bar{u}c_2]_{s=1}[\bar{d}c_1]_{s=1}\rangle_{J=0} - \frac{1}{2}|[\bar{u}c_2]_{s=0}[\bar{d}c_1]_{s=0}\rangle_{J=0}. \end{aligned} \quad (13)$$

Then the mass difference of $T_{cc}[\bar{\mathbf{3}}, {}^3S_1]_{0^+, 1^+, 2^+}^{I=1}$ from the ground state $T_{cc}[\bar{\mathbf{3}}, {}^3S_1]$ is estimated as

$$M(T_{cc}[\bar{\mathbf{3}}, {}^3S_1]_{0^+, 1^+, 2^+}^{I=1}) - M(T_{cc}[\bar{\mathbf{3}}, {}^3S_1])$$

$$\begin{aligned}
&= \left(\frac{1}{4} \frac{C_{qq}}{m_u^2} + \frac{1}{4} \frac{C_{cc}}{m_c^2} + x \frac{C_{q\bar{q}}}{m_u m_c} \right) - \left(-\frac{3}{4} \frac{C_{qq}}{m_u^2} + \frac{1}{4} \frac{C_{cc}}{m_c^2} \right) \\
&= \frac{C_{qq}}{m_u^2} + x \frac{C_{q\bar{q}}}{m_u m_c} \simeq (193 + 64x) \text{ MeV}
\end{aligned} \tag{14}$$

where $x = -1$, $-\frac{1}{2}$, and $\frac{1}{2}$ for 0^+ , 1^+ , and 2^+ , respectively. Explicitly, the corresponding values are 129 MeV, 161 MeV, and 225 MeV. The mass difference of $T_{cc}[\mathbf{6}, {}^1S_0]^{I=1}$ from $T_{cc}[\mathbf{6}, {}^1S_0]$ is

$$\begin{aligned}
M(T_{cc}[\mathbf{6}, {}^1S_0]^{I=1}) - M(T_{cc}[\mathbf{6}, {}^1S_0]) &= \left(\frac{3}{8} \frac{C_{qq}}{m_u^2} + \frac{3}{8} \frac{C_{cc}}{m_c^2} \right) - \left(-\frac{1}{8} \frac{C_{qq}}{m_u^2} + \frac{3}{8} \frac{C_{cc}}{m_c^2} \right) \\
&= \frac{1}{2} \frac{C_{qq}}{m_u^2} \simeq 96.5 \text{ MeV}.
\end{aligned} \tag{15}$$

Here, we have used the matrix elements in Table 1. One may use this method to check that there is no heavy-light correlation in the $I = 0$ states

$$\begin{aligned}
|[\bar{u}\bar{d}]_{s=0}[c_1c_2]_{s=1}\rangle_{J=1} &= \frac{1}{\sqrt{2}}|[\bar{u}c_1]_{s=1}[\bar{d}c_2]_{s=1}\rangle_{J=1} - \frac{1}{2}|[\bar{u}c_1]_{s=1}[\bar{d}c_2]_{s=0}\rangle_{J=1} \\
&\quad + \frac{1}{2}|[\bar{u}c_1]_{s=0}[\bar{d}c_2]_{s=1}\rangle_{J=1}
\end{aligned} \tag{16}$$

$$\begin{aligned}
&= \frac{1}{\sqrt{2}}|[\bar{u}c_2]_{s=1}[\bar{d}c_1]_{s=1}\rangle_{J=1} - \frac{1}{2}|[\bar{u}c_2]_{s=1}[\bar{d}c_1]_{s=0}\rangle_{J=1} \\
&\quad + \frac{1}{2}|[\bar{u}c_2]_{s=0}[\bar{d}c_1]_{s=1}\rangle_{J=1},
\end{aligned} \tag{17}$$

$$\begin{aligned}
|[\bar{u}\bar{d}]_{s=1}[c_1c_2]_{s=0}\rangle_{J=1} &= \frac{1}{\sqrt{2}}|[\bar{u}c_1]_{s=1}[\bar{d}c_2]_{s=1}\rangle_{J=1} + \frac{1}{2}|[\bar{u}c_1]_{s=1}[\bar{d}c_2]_{s=0}\rangle_{J=1} \\
&\quad - \frac{1}{2}|[\bar{u}c_1]_{s=0}[\bar{d}c_2]_{s=1}\rangle_{J=1}
\end{aligned} \tag{18}$$

$$\begin{aligned}
&= -\frac{1}{\sqrt{2}}|[\bar{u}c_2]_{s=1}[\bar{d}c_1]_{s=1}\rangle_{J=1} - \frac{1}{2}|[\bar{u}c_2]_{s=1}[\bar{d}c_1]_{s=0}\rangle_{J=1} \\
&\quad + \frac{1}{2}|[\bar{u}c_2]_{s=0}[\bar{d}c_1]_{s=1}\rangle_{J=1}.
\end{aligned} \tag{19}$$

As a result, we obtain the mass spectrum of doubly charmed tetraquarks shown in Fig. 1 (b). It is instructive to compare this spectrum with the corresponding baryon spectrum in Fig. 1 (a). The tetraquarks with color $\bar{\mathbf{3}}$ correlation have their counterpart in the baryon spectrum, while the color $\mathbf{6}$ states are only allowed in T_{cc} . The exotic color $\mathbf{6}$ correlation is a unique feature of the tetraquark state, which is not accessible in ordinary hadrons.

Because the $I = 1$ states are much heavier than the two-body decay threshold, the effect of the strong decay may be significant. For instance, the lowest thresholds in $I = 1$ sector are DD in s wave and d wave for $I(J^P) = 1(0^+)$ and $1(2^+)$, respectively, and DD* in s wave for $1(1^+)$ (see e.g. Table I in Ref. [70]). In the following, therefore, we discuss the structure and production of the $I = 0$ states.

In a separate work [71], the mixing effects between states with the same quantum numbers caused by the color-spin interaction are considered. It is found that the mass gap between the two $I(J^P) = 1(0^+)$ states changes from ~ 100 MeV to ~ 280 MeV and that between the two $I(J^P) = 0(1^+)$ states from ~ 130 MeV to ~ 190 MeV. Alternatively, the mass shift for the former states is around 90 MeV while that for the latter states is around 30 MeV. This observation means that the state mixing is small for the $I(J^P) = 0(1^+)$ tetraquarks (as expected) and is large for the $I(J^P) = 1(0^+)$ tetraquarks. As a result, the decay properties for the $I(J^P) = 1(0^+)$ states may be affected. In the following discussions, we mainly focus on the isoscalar tetraquarks $T_{cc}[\bar{\mathbf{3}}, {}^3S_1]$ and $T_{cc}[\mathbf{6}, {}^1S_0]$. When we consider the T_{cc} production, the $I(J^P) = 1(0^+)$ states will also be discussed.

2.3. Decay modes of T_{cc}

For experimental searches, it is important to specify the decay properties. Possible decay modes of $T_{cc}[\bar{\mathbf{3}}, {}^3S_1]$ and $T_{cc}[\mathbf{6}, {}^1S_0]$ are summarized in Table 2. Because $T_{cc}[\bar{\mathbf{3}}, {}^3S_1]$ is stable against the strong decay in our estimation, it can decay only by the weak and electromagnetic interactions. In contrast, $T_{cc}[\mathbf{6}, {}^1S_0]$ decays via the strong interaction which is the dominant contribution to the total width of $T_{cc}[\mathbf{6}, {}^1S_0]$. Because $T_{cc}[\mathbf{6}, {}^1S_0]$ has positive charge, the final state in the strong decay is $D^0 D^{*+}$ and/or $D^{*0} D^+$. The direct decay into DD π state (with one of the particles being positively charged) is also possible.

To consider the weak decay, we recall the rearrangement of color configuration of T_{cc} in Eqs. (5)-(8). The weak decay of T_{cc} is caused by the decay of D meson in the DD* ($D^0 D^{*+}$ or $D^{*0} D^+$) component. The final state can be, for instance, $D^* \bar{K} \pi$, $D \bar{K} \pi \pi$, $D^* \bar{K} \pi \pi \pi$, and so on. Among others, $D^{*+} K^- \pi^+$ and $D^{*+} K^- \pi^+ \pi^+ \pi^-$ are advantageous in experimental searches, because the final states are all charged particles.

The radiative decay of T_{cc} occurs through the $D^{*0} \rightarrow D^0 \gamma$ process, which is about 38 % of the D^{*0} decay [11]. According to Eqs. (5)-(8), the fraction of the DD* component is 1/3 in $T_{cc}[\bar{\mathbf{3}}, {}^3S_1]$ and 2/3 in $T_{cc}[\mathbf{6}, {}^1S_0]$. This indicates

Table 2: Possible decay modes of $T_{cc}[\bar{\mathbf{3}}, {}^3S_1]$ and $T_{cc}[\mathbf{6}, {}^1S_0]$. Weak decays with all charged final states are shown.

	$T_{cc}[\bar{\mathbf{3}}, {}^3S_1]$	$T_{cc}[\mathbf{6}, {}^1S_0]$
strong decay	—	$D^0 D^{*+}, D^{*0} D^+$ $D^0 D^0 \pi^+, D^0 D^+ \pi^0$
weak decay	$D^+ K^- \pi^+, D^{*+} K^- \pi^+, D^{*+} K^- \pi^+ \pi^+ \pi^-$	same with $T_{cc}[\bar{\mathbf{3}}, {}^3S_1]$
radiative decay	$D^+ D^0 \gamma$	same with $T_{cc}[\bar{\mathbf{3}}, {}^3S_1]$

the ratio of the radiative decays of $T_{cc}[\bar{\mathbf{3}}, {}^3S_1]$ and $T_{cc}[\mathbf{6}, {}^1S_0]$ will be

$$\frac{\text{Br}(T_{cc}[\bar{\mathbf{3}}, {}^3S_1] \rightarrow D^+ D^0 \gamma)}{\text{Br}(T_{cc}[\mathbf{6}, {}^1S_0] \rightarrow D^+ D^0 \gamma)} = \frac{1}{2}. \quad (20)$$

Thus, the measurement of the radiative decay will provide an interesting method to discriminate the internal color structures of $T_{cc}[\bar{\mathbf{3}}, {}^3S_1]$ and $T_{cc}[\mathbf{6}, {}^1S_0]$, in addition to the information from the mass spectroscopy and the production process, as discussed in section 4.

3. Wave function of tetraquark T_{cc}

In this section, we discuss the spatial wave function of tetraquark T_{cc} in the non-relativistic constituent quark model. The spatial correlation of the cc pair in T_{cc} is important to estimate the total cross section of the inclusive production of T_{cc} in the next section. We first determine the model parameters by using the masses of normal charm hadrons, and then apply the model setup to T_{cc} .

3.1. Constituent quark model with harmonic oscillator potential

As the simple model, we consider the quark model with the harmonic oscillator potential as the color confinement potential. The interaction between quarks 1 and 2 is given by

$$V_{12}(r) = \left(-\frac{3}{16} \vec{\lambda}_1 \cdot \vec{\lambda}_2 \right) \frac{k}{2} r_{12}^2, \quad (21)$$

Table 3: The expectation values of $\vec{\lambda}_1 \cdot \vec{\lambda}_2$ for $\bar{q}q$ and qq channels.

$\bar{q}q$		qq	
$\mathbf{1}_c$	$\mathbf{8}_c$	$\mathbf{3}_c$	$\mathbf{6}_c$
$-16/3$	$2/3$	$-8/3$	$4/3$

with the strength constant k and the relative distance between the two particle r_{12} . The matrix element of the color factor $\vec{\lambda}_1 \cdot \vec{\lambda}_2$ are summarized in Table 3. In Eq. (21), the strength is normalized as unity for the single $\bar{q}q$ channel. Let us consider the $q\bar{q}$ system with reduced mass μ . By defining $\mu\omega^2 = (-3/16)\langle \mathbf{1} | \vec{\lambda}_1 \cdot \vec{\lambda}_2 | \mathbf{1} \rangle k$, the Hamiltonian for this system is

$$H_{\text{HO}}(\vec{x}) = -\frac{1}{2\mu} \frac{\partial^2}{\partial \vec{x}^2} + \frac{\mu\omega^2}{2} \vec{x}^2, \quad (22)$$

where $\vec{x} = (x, y, z)$ is the relative coordinate. The solution of the Schrödinger equation is specified by the non-negative integers $\{n\} = \{n_1, n_2, n_3\}$ as

$$\varphi_{\{n\}}(x, y, z) = C_{\{n\}} e^{-\frac{\mu\omega}{2}(x^2+y^2+z^2)} H_{n_1}(\sqrt{\mu\omega}x) H_{n_2}(\sqrt{\mu\omega}y) H_{n_3}(\sqrt{\mu\omega}z) \quad (23)$$

with the Hermite polynomials H_n and a normalization constant $C_{\{n\}}$. For the ground state with $\{n\} = \{0, 0, 0\} \equiv \{0\}$, the normalized solution is given by

$$\varphi_{\{0\}}(x, y, z) = \left(\frac{\mu\omega}{\pi}\right)^{3/4} e^{-\frac{\mu\omega}{2}(x^2+y^2+z^2)}. \quad (24)$$

The root-mean-squared-radius $\sqrt{\langle \vec{x}^2 \rangle}$ for the ground state is calculated as

$$\begin{aligned} \sqrt{\langle \vec{x}^2 \rangle} &= \left[\int \varphi_{\{0\}}^*(\vec{x}) \vec{x}^2 \varphi_{\{0\}}(\vec{x}) d^3\vec{x} \right]^{1/2} \\ &= \sqrt{\frac{3}{2}} \frac{1}{\sqrt{\mu\omega}}. \end{aligned} \quad (25)$$

3.2. Parameter fitting to charmonium mass

In determination of the model parameters, what is the most important in our discussion is the value of the wave function at the center-of-mass for $c\bar{c}$ quark pair. In the realistic calculation with the Cornell (linear-type) potential by Barnes, Godfrey and Swanson [72], they obtained the values

$$|R_{\eta_c}(0)|^2 = (1.39)^2 \text{ GeV}^3, \quad (26)$$

$$|R_{J/\psi}(0)|^2 = (1.10)^2 \text{ GeV}^3, \quad (27)$$

for η_c and J/ψ , respectively. We use the averaged value in spin;

$$\frac{|R_{\eta_c}(0)|^2 + 3|R_{J/\psi}(0)|^2}{4} = (1.18)^2 \text{ GeV}^3. \quad (28)$$

In their calculation, the charm quark mass is $m_c = 1.48 \text{ GeV}$.

In our simple harmonic oscillator potential, the corresponding value is given as

$$R_{c\bar{c}}(0) = \frac{2}{b^{3/2}}, \quad (29)$$

with $b = 1/\sqrt{\mu\omega}$ from Eq. (24). When we require that $|R_{c\bar{c}}(0)|^2 = (1.18)^2 \text{ GeV}^3$ (Eq. (28)), we obtain $\omega = 0.699 \text{ GeV}$ and $k = \mu\omega^2 = 0.331 \text{ GeV}^3$. In the followings, we use this value, not only for the $c\bar{c}$ channel, but also for the cc channel. The potential for the latter is easily obtained by changing the color factor in Eq. (21).

However, there is some ambiguity in determination of the parameters, m_c and ω . We can use another way to reproduce the mass splitting between the s -wave charmonia (η_c , J/ψ) and p -wave charmonia (h_c and χ_{cJ} ($J = 0, 1, 2$)), which corresponds to the frequency ω in the harmonic oscillator potential $V(r) = (\mu\omega^2/2)r^2$. We choose $\omega = 0.295 \text{ GeV}$ with the charm quark mass $m_c = 1.326 \text{ GeV}$ ($\mu = m_c/2$) [73]. The corresponding value of the spring constant in the present potential is $k = 0.0577 \text{ GeV}^3$. In this case, we obtain $|R_{c\bar{c}}(0)|^2 = (0.59)^2 \text{ GeV}^3$. We will discuss how the results change in the production cross section of T_{cc} for different parameter sets in section 4.

3.3. T_{cc}

T_{cc} is the four-body system with the quark content $cc\bar{u}\bar{d}$. From the quark-quark interaction in Eq. (21), the Hamiltonian is given as

$$\begin{aligned} H(\vec{r}_1, \vec{r}_2, \vec{r}_3, \vec{r}_4) &= K + V \\ &= \sum_{i=1}^4 \left(-\frac{1}{2m_i} \vec{\nabla}_i^2 \right) + \left(-\frac{3}{16} \right) \frac{k}{2} \sum_{i<j} \vec{\lambda}_i \cdot \vec{\lambda}_j (\vec{r}_i - \vec{r}_j)^2, \end{aligned} \quad (30)$$

for four quarks $i = 1, 2, 3, 4$. This is our basic Hamiltonian for $T_{cc}[\bar{\mathbf{3}}, {}^3S_1]$ and $T_{cc}[\mathbf{6}, {}^1S_0]$.

3.3.1. $T_{cc}[\bar{\mathbf{3}}, {}^3S_1]$

We assume that the pair of two quarks (antiquarks) belong to color $\bar{\mathbf{3}}_c$ ($\mathbf{3}_c$). In the four-body system, however, we cannot single out the color factor $\vec{\lambda}_i \cdot \vec{\lambda}_j$, because it acts not only to the *quark-quark* pair with $\bar{\mathbf{3}}_c$ but also the *quark-antiquark* pair with $\mathbf{1}_c$ or $\mathbf{8}_c$. Then, we obtain the values of the color factor $\vec{\lambda}_i \cdot \vec{\lambda}_j$ ($i < j$);

$$\begin{aligned} \vec{\lambda}_1 \cdot \vec{\lambda}_2 &= -\frac{8}{3}, \\ \vec{\lambda}_1 \cdot \vec{\lambda}_3 &= \frac{1}{3} \left(-\frac{16}{3} \right) + \frac{2}{3} \frac{2}{3} = -\frac{4}{3}, \\ \vec{\lambda}_1 \cdot \vec{\lambda}_4 &= \frac{1}{3} \left(-\frac{16}{3} \right) + \frac{2}{3} \frac{2}{3} = -\frac{4}{3}, \\ \vec{\lambda}_2 \cdot \vec{\lambda}_3 &= \frac{1}{3} \left(-\frac{16}{3} \right) + \frac{2}{3} \frac{2}{3} = -\frac{4}{3}, \\ \vec{\lambda}_2 \cdot \vec{\lambda}_4 &= \frac{1}{3} \left(-\frac{16}{3} \right) + \frac{2}{3} \frac{2}{3} = -\frac{4}{3}, \\ \vec{\lambda}_3 \cdot \vec{\lambda}_4 &= -\frac{8}{3}, \end{aligned} \quad (31)$$

which are obtained by $\langle \mathbf{3}_{12} \bar{\mathbf{3}}_{34} | \vec{\lambda}_i \cdot \vec{\lambda}_j | \mathbf{3}_{12} \bar{\mathbf{3}}_{34} \rangle$ with using Eqs. (5) and (6). As a consequence, the potential in Eq. (30) becomes

$$\begin{aligned} V &= \frac{k}{2} \left\{ \frac{1}{2} (\vec{r}_1 - \vec{r}_2)^2 + \frac{1}{4} (\vec{r}_1 - \vec{r}_3)^2 + \frac{1}{4} (\vec{r}_1 - \vec{r}_4)^2 \right. \\ &\quad \left. + \frac{1}{4} (\vec{r}_2 - \vec{r}_3)^2 + \frac{1}{4} (\vec{r}_2 - \vec{r}_4)^2 + \frac{1}{2} (\vec{r}_3 - \vec{r}_4)^2 \right\}. \end{aligned} \quad (32)$$

Now, let us introduce the relative coordinates $\vec{\xi}$, $\vec{\eta}$ and $\vec{\zeta}$ and the center-of-mass coordinate \vec{R} , which are defined by

$$\begin{pmatrix} \vec{\xi} \\ \vec{\eta} \\ \vec{\zeta} \\ \vec{R} \end{pmatrix} = \begin{pmatrix} 1 & -1 & 0 & 0 \\ \frac{m_1}{m_{12}} & \frac{m_2}{m_{12}} & -1 & 0 \\ \frac{m_1}{m_{123}} & \frac{m_2}{m_{123}} & \frac{m_3}{m_{123}} & -1 \\ \frac{m_1}{M} & \frac{m_2}{M} & \frac{m_3}{M} & \frac{m_4}{M} \end{pmatrix} \begin{pmatrix} \vec{r}_1 \\ \vec{r}_2 \\ \vec{r}_3 \\ \vec{r}_4 \end{pmatrix}, \quad (33)$$

with the original coordinate \vec{r}_i for the (anti)particle i . Here we define $m_{12} = m_1 + m_2$, $m_{123} = m_1 + m_2 + m_3$ and $M = m_1 + m_2 + m_3 + m_4$ (the center-of-mass). The kinetic term is then rewritten as

$$K = -\frac{1}{2\mu} \vec{\nabla}_{\xi}^2 - \frac{1}{2\nu} \vec{\nabla}_{\eta}^2 - \frac{1}{2\rho} \vec{\nabla}_{\zeta}^2 - \frac{1}{2M} \vec{\nabla}_R^2, \quad (34)$$

where we define the reduced masses

$$\mu = \frac{m_1 m_2}{m_{12}}, \quad (35)$$

$$\nu = \frac{m_{12} m_3}{m_{123}}, \quad (36)$$

$$\rho = \frac{m_{123} m_4}{M}. \quad (37)$$

The potential term is also rewritten as

$$\begin{aligned} V = & \frac{k}{2} \left\{ \left(\frac{1}{2} + \frac{1}{2} \frac{m_1^2 + m_2^2}{m_{12}^2} \right) \vec{\xi}^2 + \left(\frac{1}{2} + \frac{1}{2} \frac{m_{12}^2 + m_3^2}{m_{123}^2} \right) \vec{\eta}^2 + \vec{\zeta}^2 \right. \\ & + \frac{1}{2} \left(\frac{-m_1 + m_2}{m_{12}} + \frac{-m_1 + m_2}{m_{12}} \frac{m_3}{m_{123}} \right) \vec{\xi} \cdot \vec{\zeta} \\ & \left. + \frac{1}{2} \frac{-m_1 + m_2}{m_{12}} \vec{\xi} \cdot \vec{\zeta} + \left(\frac{-m_1 - m_2 + m_3}{m_{123}} \right) \vec{\eta} \cdot \vec{\zeta} \right\}. \end{aligned} \quad (38)$$

Interestingly, for $m_1 = m_2$, the relative coordinate $\vec{\xi}$ is decoupled from $\vec{\eta}$ and $\vec{\zeta}$ completely.⁵ This is the special property for the harmonic oscillator

⁵There is still a coupling for $\vec{\eta}$ and $\vec{\zeta}$. However, this coupling is irrelevant to the estimation of the wave function of cc quark pair as discussed below.

potential in Eq. (21). For the cc pair (assigned as the particle 1 and 2) described by $\vec{\xi}$, we obtain the Hamiltonian for $\vec{\xi}$

$$H_{\xi}^{\text{T}_{\text{cc}}[\bar{\mathbf{3}}, {}^3\text{S}_1]} = -\frac{1}{2\mu}\vec{\nabla}_{\xi}^2 + \frac{3}{4}\frac{k}{2}\vec{\xi}^2, \quad (39)$$

which happens to be the same Hamiltonian for the cc pair in Ξ_{cc} .⁶ Consequently, we obtain the value of the wave function at the center-of-mass of the cc pair in $\text{T}_{\text{cc}}[\bar{\mathbf{3}}, {}^3\text{S}_1]$

$$R_{\text{cc}}^{\text{T}_{\text{cc}}[\bar{\mathbf{3}}, {}^3\text{S}_1]}(0) = \frac{2}{b^{3/2}} = 1.06 \text{ GeV}^{3/2}, \quad (41)$$

with $b = 1/\sqrt{\mu\omega}$ and $\omega = \sqrt{3/4}\sqrt{k/\mu}$ for $k = 0.331 \text{ GeV}^3$ and $\mu = m_c/2 = 1.48/2 \text{ GeV}$.

3.3.2. $\text{T}_{\text{cc}}[\mathbf{6}, {}^1\text{S}_0]$

Next, we consider the case that the pair of two quarks (antiquarks) belongs to $\mathbf{6}_c$. Using the values of $\vec{\lambda}_i \cdot \vec{\lambda}_j$ ($i < j$) as

$$\begin{aligned} \vec{\lambda}_1 \cdot \vec{\lambda}_2 &= \frac{4}{3}, \\ \vec{\lambda}_1 \cdot \vec{\lambda}_3 &= \frac{2}{3} \left(-\frac{16}{3} \right) + \frac{1}{3} \frac{2}{3} = -\frac{10}{3}, \\ \vec{\lambda}_1 \cdot \vec{\lambda}_4 &= \frac{2}{3} \left(-\frac{16}{3} \right) + \frac{1}{3} \frac{2}{3} = -\frac{10}{3}, \\ \vec{\lambda}_2 \cdot \vec{\lambda}_3 &= \frac{2}{3} \left(-\frac{16}{3} \right) + \frac{1}{3} \frac{2}{3} = -\frac{10}{3}, \\ \vec{\lambda}_2 \cdot \vec{\lambda}_4 &= \frac{2}{3} \left(-\frac{16}{3} \right) + \frac{1}{3} \frac{2}{3} = -\frac{10}{3}, \\ \vec{\lambda}_3 \cdot \vec{\lambda}_4 &= \frac{4}{3}, \end{aligned} \quad (42)$$

⁶In case of Ξ_{cc} , we consider the three-body system ccq and find that the Hamiltonian for cc quark pair is given by

$$H_{\xi}^{\Xi_{\text{cc}}} = -\frac{1}{2\mu}\vec{\nabla}_{\xi}^2 + \frac{3}{4}\frac{k}{2}\vec{\xi}^2, \quad (40)$$

with the relative coordinate $\vec{\xi}$ for cc distance, which turns out to be the same as Eq. (39).

we obtain the potential given by

$$\begin{aligned}
V = & \frac{k}{2} \left\{ \left(-\frac{1}{4} + \frac{5}{4} \frac{m_1^2 + m_2^2}{m_{12}^2} \right) \vec{\xi}^2 + \left(\frac{5}{4} + \frac{1}{4} \frac{-m_{12}^2 + 5m_3^2}{m_{123}^2} \right) \vec{\eta}^2 + \vec{\zeta}^2 \right. \\
& + 2 \left(\frac{5 - m_1 + m_2}{8} \frac{1}{m_{12}} + \frac{5 - m_1 + m_2}{8} \frac{m_3}{m_{12} m_{123}} \right) \vec{\xi} \cdot \vec{\eta} \\
& \left. + 2 \frac{5 - m_1 + m_2}{8} \frac{1}{m_{12}} \vec{\xi} \cdot \vec{\zeta} + 2 \frac{1}{4} \frac{m_{12} + 5m_3}{m_{123}} \vec{\eta} \cdot \vec{\zeta} \right\}, \quad (43)
\end{aligned}$$

where the relative coordinate in Eq. (33) is used. For the case of $m_1 = m_2$, the relative coordinate $\vec{\xi}$ for the cc pair is decoupled from $\vec{\eta}$ and $\vec{\zeta}$ decoupled again, and hence we obtain the Hamiltonian

$$H_{\xi}^{\text{T}_{\text{cc}}[\mathbf{6},^1\text{S}_0]} = -\frac{1}{2\mu} \vec{\nabla}_{\xi}^2 + \frac{3k}{8} \frac{1}{2} \xi^2, \quad (44)$$

for the cc pair. Consequently, we get the value of the wave function at the center-of-mass of the cc pair in $\text{T}_{\text{cc}}(\mathbf{6}_c)$

$$R_{\text{cc}}^{\text{T}_{\text{cc}}[\mathbf{6},^1\text{S}_0]}(0) = \frac{2}{b^{3/2}} = 0.817 \text{ GeV}^{3/2}, \quad (45)$$

with $b = 1/\sqrt{\mu\omega}$ and $\omega = \sqrt{3/8} \sqrt{k/\mu}$ for $k = 0.331 \text{ GeV}^3$ and $\mu = m_c/2 = 1.48/2 \text{ GeV}$ (Set A). The value for $\text{T}_{\text{cc}}[\mathbf{6},^1\text{S}_0]$ is smaller than that for $\text{T}_{\text{cc}}[\mathbf{\bar{3}},^3\text{S}_1]$. This is indeed the case, because the potential strength in Eq. (44) is half as small as that in Eq. (39). We show also the result for $k = 0.0577 \text{ GeV}^3$ and $\mu = m_c/2 = 1.326 \text{ GeV}$ from the mass splittings of s -wave and p -wave charmonia (Set B). The summary of the present result for $R_{\text{cc}}(0)$ is given in Table. 4. Those values will be used in the estimation of the T_{cc} production in the next section.

4. Inclusive production of tetraquark T_{cc}

To pin down the properties of exotic color configurations of T_{cc} , it is important to relate the internal structure of T_{cc} to some experimental observables. Because the T_{cc} production requires at least two $c\bar{c}$ pairs, low energy exclusive production is not very promising. Refs. [51–53] have discussed the production of T_{cc} in heavy ion collisions where charm quark pairs are produced abundantly. Here we consider the inclusive T_{cc} production

Table 4: The values of the wave function at the center-of-mass $R_{cc}(0)$ for the cc pair in $T_{cc}[\bar{\mathbf{3}}, {}^3S_1]$ and $T_{cc}[\mathbf{6}, {}^1S_0]$, respectively. Units are $\text{GeV}^{3/2}$.

	Set A	Set B
$T_{cc}[\bar{\mathbf{3}}, {}^3S_1]$	1.06	0.53
$T_{cc}[\mathbf{6}, {}^1S_0]$	0.82	0.41

in electron-positron collisions. In fact, the double-charm productions with charmonia in the final state are analyzed at Belle and BaBar [54–56]. In this section, we introduce the theoretical framework to describe the T_{cc} production.

4.1. NRQCD framework

To evaluate the production of T_{cc} , we utilize the non-relativistic QCD (NRQCD) [63, 64], which is an effective field theory for heavy quarks. This framework allows one to factorize the hard part of the process in which the heavy quarks are produced at short distance and the soft part where the heavy quarks fragment into hadrons. The hard process is calculable through the matching of the NRQCD operator with the perturbative QCD amplitude as an expansion of α_s . The soft part is given by the nonperturbative matrix elements of the NRQCD operators expanded in powers of the heavy quark velocity v .

NRQCD was originally introduced to describe the annihilation decay and the production of single charmonium, and was later applied to double-charm productions with charmonia in the final states [74–76, 78, 79]. It was shown that the higher order corrections both in α_s [79] and velocity expansion [78] are important for the double-charmonium productions.

For the inclusive T_{cc} production in electron-positron collisions ($e^+e^- \rightarrow T_{cc}[\alpha] + X$), the differential cross section is given by

$$\begin{aligned}
& d\sigma_\alpha(e^+e^- \rightarrow T_{cc}[\alpha] + X) \\
&= \sum_k d\hat{\sigma}(e^+e^- \rightarrow [cc]_\alpha^k + \bar{c} + \bar{c}) \langle \mathcal{O}^k(T_{cc}[\alpha]) \rangle \\
&= \sum_k d\hat{\sigma}(e^+e^- \rightarrow [cc]_\alpha^k + \bar{c} + \bar{c}) |\langle T_{cc}[\alpha] + X' | [cc]_\alpha^k | 0 \rangle|^2, \quad (46)
\end{aligned}$$

where α stands for the color-spin configuration of cc pair inside T_{cc} , k indicates the order of the velocity expansion, and X' represents the light components nonperturbatively produced during the soft hadronization process of the cc pair to the T_{cc} state. $d\hat{\sigma}$ is the cross section for the elementary process $e^+e^- \rightarrow [cc]_\alpha^k + \bar{c} + \bar{c}$, where the cc pair is combined to form the color-spin configuration α at order k . As a first trial, here we consider the leading order calculation both in α_s and v . In this case, the nonperturbative matrix element is a number for each α and we denote it as

$$|\langle T_{cc}[\alpha] + X' |[cc]_\alpha^k | 0 \rangle|^2 \Big|_{k=\text{LO}} = \begin{cases} h_{[\bar{\mathbf{3}}, {}^3S_1]} & \text{for } \alpha = [\bar{\mathbf{3}}, {}^3S_1], \\ h_{[\mathbf{6}, {}^1S_0]} & \text{for } \alpha = [\mathbf{6}, {}^1S_0]. \end{cases} \quad (47)$$

In the following, we first present the kinematics of the reaction in Section 4.2, and then show the calculation of the hard process in Section 4.3. The treatment of the soft matrix element is discussed in Section 4.4.

4.2. Kinematics

We assign momentum variables as $e^+(p_1)e^-(p_2) \rightarrow [cc]_\alpha^k(p) + \bar{c}(p_3) + \bar{c}(p_4)$. We choose the collision axis as the z direction in the center of mass frame, and x axis is set so that T_{cc} moves in the xz plane. We write the magnitude of the three-momentum \mathbf{p} as p and the angle of \mathbf{p} from the z axis as Θ . The momenta of anticharm quarks are given by $\mathbf{p}_3 = -\mathbf{p}/2 + \mathbf{q}$ and $\mathbf{p}_4 = -\mathbf{p}/2 - \mathbf{q}$ with $\mathbf{q} = (\tilde{q} \sin \theta, q_y, \tilde{q} \cos \theta)$ in the cylindrical polar coordinates. These momenta and the coordinate system are summarized in Fig. 2. The four velocities of the system are then written as

$$p_1^\mu = (E_1, 0, 0, \frac{\sqrt{s}}{2}), \quad (48)$$

$$p_2^\mu = (E_2, 0, 0, -\frac{\sqrt{s}}{2}), \quad (49)$$

$$p^\mu = (E_p, p \sin \Theta, 0, p \cos \Theta), \quad (50)$$

$$p_3^\mu = (E_3, -\frac{p}{2} \sin \Theta + \tilde{q} \sin \theta, q_y, -\frac{p}{2} \cos \Theta + \tilde{q} \cos \theta), \quad (51)$$

$$p_4^\mu = (E_4, -\frac{p}{2} \sin \Theta - \tilde{q} \sin \theta, -q_y, -\frac{p}{2} \cos \Theta - \tilde{q} \cos \theta), \quad (52)$$

where s is the total energy squared. We neglect the electron mass, and regard the mass of T_{cc} as $2m_c$ in the leading order of the velocity expansion. The

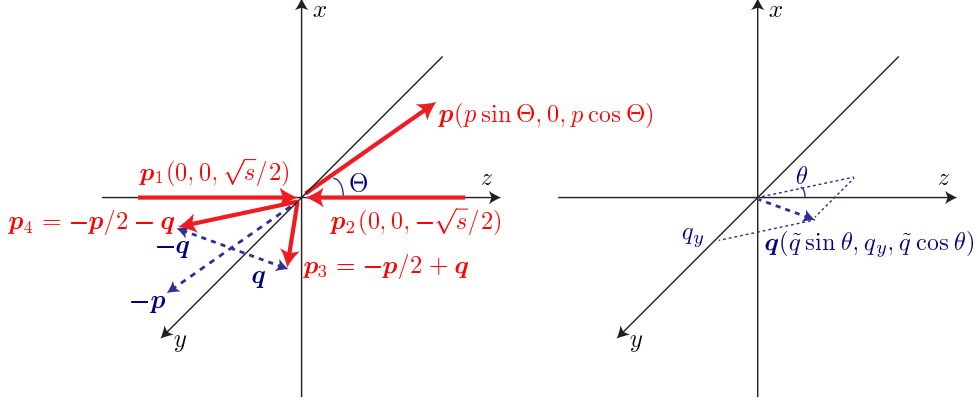


Figure 2: Assignment of the momentum variables of the inclusive T_{cc} production in the center of mass frame.

energies are then given by

$$E_1 = \frac{\sqrt{s}}{2}, \quad (53)$$

$$E_2 = \frac{\sqrt{s}}{2}, \quad (54)$$

$$E_p = \sqrt{4m_c^2 + p^2}, \quad (55)$$

$$E_3 = \sqrt{m_c^2 + \frac{p^2}{4} + \tilde{q}^2 + q_y^2 - p\tilde{q}\cos(\theta - \Theta)}, \quad (56)$$

$$E_4 = \sqrt{m_c^2 + \frac{p^2}{4} + \tilde{q}^2 + q_y^2 + p\tilde{q}\cos(\theta - \Theta)}, \quad (57)$$

With the above setup, the total cross section is given by

$$\begin{aligned} \sigma_\alpha = & \frac{1}{2} \frac{1}{2s} \frac{1}{m_c} \int \frac{d^3p}{(2\pi)^3} \frac{1}{2E_p} \frac{d^3p_3}{(2\pi)^3} \frac{1}{2E_3} \frac{d^3p_4}{(2\pi)^3} \frac{1}{2E_4} \\ & \times (2\pi)^4 \delta^4(p_1 + p_2 - p - p_3 - p_4) \overline{\sum} |\hat{\mathcal{M}}_\alpha|^2 h_\alpha, \end{aligned} \quad (58)$$

where $\overline{\sum} |\hat{\mathcal{M}}_\alpha|^2$ stands for the color-spin projected squared amplitude with the summation over the final spins and average over the initial spins. The factor $1/2$ is the symmetry factor of identical \bar{c} quarks in the final state, and $1/m_c$ comes from the non-relativistic normalization of the state vector in the matrix element h_α . Performing the phase space integration, we obtain the differential cross section with respect to the T_{cc} momentum p and scattered

angle $\cos \Theta$ as

$$\frac{d\sigma_\alpha}{dp \, d\cos \Theta} = \frac{1}{(2\pi)^4} \frac{p^2}{16sE_p m_c} \int_0^{2\pi} d\theta \int_0^{\tilde{q}_{\max}} d\tilde{q} \frac{\tilde{q}}{q_y(E_3 + E_4)} \overline{\sum} |\hat{\mathcal{M}}_\alpha|^2 h_\alpha, \quad (59)$$

where we define

$$q_y = \frac{\sqrt{A - B\tilde{q}^2 + C\tilde{q}^2 \cos^2(\theta - \Theta)}}{2(\sqrt{s} - E_p)}, \quad (60)$$

$$\tilde{q}_{\max} = \sqrt{\frac{A}{B - C \cos^2(\theta - \Theta)}}, \quad (61)$$

with $A = \sqrt{s}(\sqrt{s} - 2E_p)(\sqrt{s} - E_p)^2$, $B = 4(\sqrt{s} - E_p)^2$, and $C = 4p^2$. Although it seems that the integrand diverges ($q_y \rightarrow 0$) when $\tilde{q} \rightarrow \tilde{q}_{\max}$, this is not a real singularity and can be removed by the transformation of the integration variable as $x^2 = \tilde{q}_{\max} - \tilde{q}$ in practice.

4.3. Perturbative QCD process

In the leading order of α_s , the perturbative amplitude for the $e^+e^- \rightarrow [cc]_\alpha^k + \bar{c} + \bar{c}$ process $\hat{\mathcal{M}}_\alpha$ is expressed by four diagrams shown in Fig. 3. The explicit forms of these amplitudes are given by

$$-i\hat{\mathcal{M}}_\alpha = -i\hat{\mathcal{M}}_\alpha^{(a)} - i\hat{\mathcal{M}}_\alpha^{(a')} - i\hat{\mathcal{M}}_\alpha^{(b)} - i\hat{\mathcal{M}}_\alpha^{(b')}, \quad (62)$$

with

$$\begin{aligned} -i\hat{\mathcal{M}}_\alpha^{(a)} &= \bar{v}_e(p_1)(ie\gamma^\mu)u_e(p_2) \frac{-ig_{\mu\nu}}{(p_1 + p_2)^2} \\ &\times v_l^t(p_3)(-ie_c(\gamma^\nu)^t) \left(\frac{i}{\not{p} + \not{p}_4 - m_c} \right)^t (-ig(\gamma^\rho)^t(T^a)_{lk}) \\ &\times [P_{\alpha,m}]_{kj} \frac{-ig_{\rho\sigma}\delta^{ab}}{(p/2 + p_4)^2} (-ig\gamma^\sigma)(T^b)_{ji} v_i(p_4), \end{aligned} \quad (63)$$

$$\begin{aligned} -i\hat{\mathcal{M}}_\alpha^{(a')} &= \bar{v}_e(p_1)(ie\gamma^\mu)u_e(p_2) \frac{-ig_{\mu\nu}}{(p_1 + p_2)^2} \\ &\times v_i^t(p_4)(-ie_c\gamma^\nu)^t \left(\frac{i}{\not{p} + \not{p}_3 - m_c} \right)^t (-ig\gamma^\rho)^t(T^a)_{ik} \\ &\times [P_{\alpha,m}]_{kj} \frac{-i\delta^{ab}g_{\rho\sigma}}{(p/2 + p_3)^2} (ig\gamma^\sigma)(T^b)_{jl} v_l(p_3), \end{aligned} \quad (64)$$

$$\begin{aligned}
-i\hat{\mathcal{M}}_\alpha^{(b)} &= ie e_c g^2 \bar{v}_e(p_1) \gamma^\mu u_e(p_2) \frac{g_{\mu\nu}}{(p_1 + p_2)^2} \\
&\times v_i^t(p_3) (\gamma^\rho)^t (T^a)_{lk}^t \left(\frac{1}{-\not{p}/2 - \not{p}_3 - \not{p}_4 - m_c} \right)^t (\gamma^\nu)^t \\
&\times [P_{\alpha,m}]_{kj} \frac{\delta^{ab} g_{\rho\sigma}}{(p/2 + p_4)^2} \gamma^\sigma (T^b)_{ji} v_i(p_4), \tag{65}
\end{aligned}$$

$$\begin{aligned}
-i\hat{\mathcal{M}}_\alpha^{(b')} &= -ie e_c g^2 \bar{v}_e(p_1) \gamma^\mu u_e(p_2) \frac{g_{\mu\nu}}{(p_1 + p_2)^2} \\
&\times v_i^t(p_4) (\gamma^\rho)^t (T^a)_{lk}^t \left(\frac{1}{-\not{p}/2 - \not{p}_3 - \not{p}_4 - m_c} \right)^t (\gamma^\nu)^t \\
&\times [P_{\alpha,m}]_{kj} \frac{\delta^{ab} g_{\rho\sigma}}{(p/2 + p_3)^2} \gamma^\sigma (T^b)_{jl} v_l(p_3), \tag{66}
\end{aligned}$$

where u_e, v_e are the electron and positron fields, u_i, v_i are the charm quark and antiquark fields with color i , and $e_c = 2e/3$ is the charge of the charm quark. The color-spin projection operators $P_{\alpha,m}$ are defined as

$$P_{\bar{\mathbf{3}},m}^{(\lambda)} = \sum_{\bar{\mathbf{3}},^3S_1} \bar{u}_k^t(p/2) \bar{u}_j(p/2) = \frac{1}{\sqrt{2}} \left(\frac{\not{p}}{2} + m_c \right)^t \not{\epsilon}^{(\lambda)t} C \Phi_{mkj}^A, \tag{67}$$

$$P_{\mathbf{6},m} = \sum_{\mathbf{6},^1S_0} \bar{u}_k^t(p/2) \bar{u}_j(p/2) = \frac{1}{\sqrt{2}} \left(\frac{\not{p}}{2} + m_c \right)^t \gamma_5 C \Phi_{mkj}^S, \tag{68}$$

where C is the charge conjugation matrix, $\epsilon_\mu^{(\lambda)}$ is the polarization vector of spin triplet T_{cc} , and $\Phi_{mkj}^{A,S} = \mp \Phi_{mjk}^{A,S}$ are the normalized tensors in color space.⁷ The suffix m specifies the color of T_{cc} , which runs 1-3 (4-9) for color $\bar{\mathbf{3}}$ ($\mathbf{6}$). The antisymmetric part is related to the Levi-Civita symbol $\Phi_{mkj}^A = \epsilon_{mkj}/\sqrt{2}$. The factor $1/\sqrt{m_c}$ is introduced to account for the normalization of the state vector $|T_{cc}[\alpha] + X_N\rangle$.

Calculating the squared amplitude, we obtain the expression with m_c and products of p_1, p_2, p, p_3 and p_4 . For instance, we have

$$\begin{aligned}
\overline{\sum} |\hat{\mathcal{M}}_\alpha^{(a)}|^2 &= \frac{2e^2 e_c^2 g^4}{3m_c (p_1 \cdot p_2)^2 (2m_c^2 + p \cdot p_4)^4} \left[4m_c^4 p \cdot p_1 p_2 \cdot p_3 \right. \\
&\quad \left. + 4m_c^2 p \cdot p_2 p_1 \cdot p_3 (m_c^2 + p \cdot p_4) + 4m_c^2 p \cdot p_1 p \cdot p_4 p_2 \cdot p_3 \right]
\end{aligned}$$

⁷In Ref. [62], transpose of the $(\not{p}/2 + m_c)$ factor has been missed as typos.

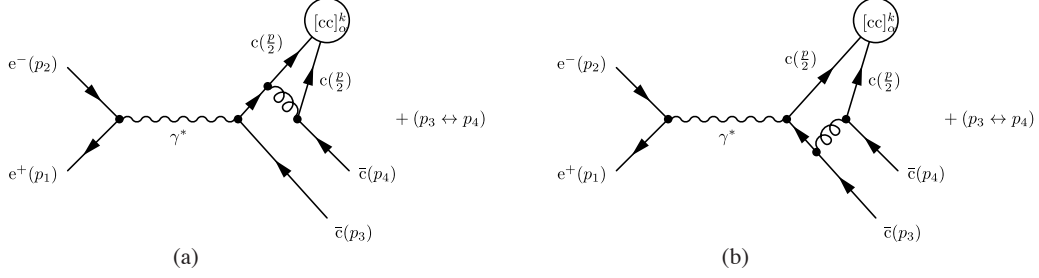


Figure 3: Feynman diagrams for the leading order contributions to the perturbative $d\hat{\sigma}(e^+e^- \rightarrow [cc]_\alpha^k + \bar{c} + \bar{c})$ process.

$$\begin{aligned}
& +4m_c^2 p \cdot p_4 p_1 \cdot p_4 p_2 \cdot p_3 + 4m_c^2 p \cdot p_4 p_1 \cdot p_3 p_2 \cdot p_4 \\
& -p_1 \cdot p_2 (8m_c^6 + 8m_c^4 p \cdot p_4 + 3m_c^2 (p \cdot p_4)^2) \\
& + (p \cdot p_4)^2 p_1 \cdot p_4 p_2 \cdot p_3 + (p \cdot p_4)^2 p_1 \cdot p_3 p_2 \cdot p_4 \Big], \quad (69)
\end{aligned}$$

for $[\alpha] = [6, {}^1S_0]$ case. Using the kinematics given in Section 4.2, we can write the squared amplitude in terms of $\sqrt{s}, p, \Theta, \tilde{q}, q_y, \theta$, which is substituted into Eq. (59) to calculate the differential cross sections.

4.4. Nonperturbative matrix element

In order to estimate the absolute values of the production cross sections in Eq. (47), we need to evaluate the soft matrix elements, which describe “fragmentation” of cc into T_{cc} .

So far, we have computed the hard part of the reaction, which produces charm quarks, *i.e.*, $e^+ + e^- \rightarrow cc + (\text{anything})$. The hard part is followed by soft hadronization processes. We here assume that the soft parts can be factorized and are given by matrix elements of final-state hadrons. For heavy quarks, one may regard the soft part as the probability of finding two charm quarks at the origin in the hadron, *i.e.*, $\propto |\psi_{cc}(0)|^2$, where $\psi_{cc}(0)$ is the relative wave function of cc in T_{cc} . Thus, we may use the expectation value at center-of-mass for the wave functions of the cc quark pairs in T_{cc} by assigning $h_{[\bar{3}, {}^3S_1]}$ and $h_{[6, {}^1S_0]}$ to $|R_{cc}^{T_{cc}[\bar{3}, {}^3S_1]}(0)|^2/4\pi$ and $|R_{cc}^{T_{cc}[6, {}^1S_0]}(0)|^2/4\pi$, respectively, as introduced in our previous work [62]. However, this is not enough for qualitative estimations, because no dynamical information to pick up light quarks from vacuum is involved. Otherwise, if one supposed no extra factor for light quarks in forming T_{cc} , then the production rates of Ξ_{cc} and T_{cc} would be of the same order. Namely, it is as easy to produce T_{cc} as Ξ_{cc} , although T_{cc} requires more light quarks, (u and d), than Ξ_{cc} does.

This observation clearly contradicts with our expectations. Including the probability of picking up light quarks to form a hadron X , $\text{Prob}(cc \rightarrow X)$, we now estimate the matrix elements as

$$h_{[\bar{\mathbf{3}},^3S_1]} = \text{Prob}(cc \rightarrow \Xi_{cc}) \times |R_{cc}^{\Xi_{cc}}(0)|^2/4\pi, \quad (70)$$

$$h_{[\mathbf{6},^1S_0]} = \text{Prob}(cc \rightarrow T_{cc}[\bar{\mathbf{3}},^3S_1]) \times |R_{cc}^{T_{cc}[\bar{\mathbf{3}},^3S_1]}(0)|^2/4\pi, \quad (71)$$

$$h_{[\mathbf{6},^1S_0]} = \text{Prob}(cc \rightarrow T_{cc}[\mathbf{6},^1S_0]) \times |R_{cc}^{T_{cc}[\mathbf{6},^1S_0]}(0)|^2/4\pi. \quad (72)$$

We thus need to take into account the probability of picking up light quarks (from vacuum) to form the final hadron. A similar situation is found in the production of heavy baryons and mesons, and it is useful for us to investigate the situations for those known hadrons. Let us compare the productions of D/B ($Q\bar{q}$) with those of Λ_Q, Σ_Q (Qqq), because the analogous investigation can be applied for Ξ_{QQ} (QQq) and T_{QQ} ($Q^2\bar{q}^2$) by regarding QQ as Q . High energy production of b quark is followed by the fragmentation into B mesons and bottom baryons, eventually decaying via the weak interaction. Fragmentation probabilities of B_u, B_d, B_s, Λ_b productions were measured at LEP (Z decay) [80, 81], CDF ($p\bar{p}$) [82, 83], and LHCb (pp) [84].

The most recent results from the LHCb [84] show the ratios,

$$\begin{aligned} \frac{f_{ud}}{f_u + f_d} &= (0.404 \pm 0.017(\text{stat}) \pm 0.027(\text{syst}) \pm 0.105(\text{Br}) \\ &\times (1 - (0.031 \pm 0.004(\text{stat}) \pm 0.003(\text{syst}) \times p_T[\text{GeV}]), \end{aligned} \quad (73)$$

where $f_{u,d,ud}$ are probabilities of b -quark fragmentation into $B^-(b\bar{u}), B^0(b\bar{d})$, and $\Lambda_b(bud)$, respectively. It should be noted that because the preceding strong decays are included, the above data includes the production probabilities from the excited states, B^* and $\Sigma_b^{(*)}$ (Σ_b and Σ_b^*), as well as the ground states, B and Λ_b :

$$f_u + f_d = \text{Prob}(b \rightarrow B + B^* + \text{other excited states}), \quad (74)$$

$$f_{ud} = \text{Prob}(b \rightarrow \Lambda_b + \Sigma_b + \Sigma_b^* + \text{other excited states}), \quad (75)$$

Measurements of the b -quark fragmentation fractions in $p\bar{p}$ collisions at $\sqrt{s} = 1.8$ TeV and 1.96 TeV were reported by the CDF Collaboration [83], giving

$$\frac{f_{ud}}{f_u + f_d} = 0.281 \pm 0.012(\text{stat})_{-0.056}^{+0.058}(\text{sys})_{-0.087}^{+0.128}(\mathcal{B}). \quad (76)$$

For understanding of b -quark fragmentation, here we heuristically assume the following simple model to calculate the ratios of production rates.

- (1) The leading heavy quark picks up light quarks and forms a heavy hadron. The light quarks are created as a quark-antiquark pair, whose “probability” is universal to all the processes.
- (2) The hadrons are produced only when the heavy quarks meet light quarks (or antiquarks) with the matched quantum numbers.

More intuitively, $q\bar{q}$ can be created in the color singlet, spin singlet 0^+ state. The pairs $u\bar{u}$ and $d\bar{d}$ are created with the same probability, while $s\bar{s}$ may be partially suppressed due to the small breaking of flavor symmetry.

Now, let us suppose the probability of creating a $u\bar{u}$ pair from the vacuum is η_u . Then the probability of creating $\bar{u}(\bar{R}, \downarrow)$ with color anti-red and spin down is $(1/6)\eta_u$. For a heavy quark $Q(R, \uparrow)$ to form a $Q\bar{u}$ ($J^\pi = 0^-$) meson, the probability is given by $(1/3)(1/2)(1/6)\eta_u = (1/36)\eta_u$, where $1/3$ is the factor for the color singlet combination, $1/2$ is for spin 0. Similarly, for the vector $Q\bar{u}$ (1^-) meson, it is $(1/3)(3/2)(1/6)\eta_u = (1/12)\eta_u$.

We obtain the same probabilities for $Q\bar{d}$ mesons, assuming $\eta_q = \eta_u = \eta_d$, and, in total, the probability of producing $B + B^*$ will be

$$f_u + f_d \sim \frac{2}{9}\eta_q. \quad (77)$$

Here we neglect the higher excited states in the total production rate.

Next, the production of baryons are estimated similarly by

$$\text{Prob}(b \rightarrow \Lambda_b) \sim \frac{1}{108}\eta_q^2, \quad (78)$$

$$\text{Prob}(b \rightarrow \Sigma_b) \sim \frac{1}{36}\eta_q^2, \quad (79)$$

$$\text{Prob}(b \rightarrow \Sigma_b^*) \sim \frac{1}{18}\eta_q^2, \quad (80)$$

and, neglecting the higher excited state, we obtain f_B as the sum,

$$f_{ud} = \frac{5}{54}\eta_q^2. \quad (81)$$

Note that the baryon will be formed by picking two light quarks and then the probability is proportional to η_q^2 .

Thus our estimate of the production ratios of the heavy baryons and heavy mesons is

$$\frac{f_{ud}}{f_u + f_d} = \frac{5}{12}\eta_q. \quad (82)$$

By using the experimental data for the ratio, $0.3 \sim 0.4$, we estimate

$$\eta_q = 0.7 \sim 1.0. \quad (83)$$

In the numerical calculation, we adopt $\eta_q = 1$.

Once η_q is obtained, we may evaluate the production probabilities of T_{cc} and Ξ_{cc} in a similar way. We obtain the production probabilities of Ξ_{cc} ($J = 1/2$) and Ξ_{cc}^* ($J = 3/2$) as

$$\text{Prob} (cc \rightarrow \Xi_{cc}) \sim \frac{1}{3} \frac{2}{3} \frac{1}{6} \eta_q = \frac{1}{27} \eta_q, \quad (84)$$

$$\text{Prob} (cc \rightarrow \Xi_{cc}^*) \sim \frac{1}{3} \frac{4}{3} \frac{1}{6} \eta_q = \frac{2}{27} \eta_q. \quad (85)$$

The production probabilities of T_{cc} are also given by

$$\text{Prob} (cc \rightarrow T_{cc}[\bar{\mathbf{3}}, {}^3S_1]) \sim \frac{1}{108} \eta_q^2, \quad (86)$$

$$\text{Prob} (cc \rightarrow T_{cc}[\mathbf{6}, {}^1S_0]) \sim \frac{1}{72} \eta_q^2, \quad (87)$$

for $I = 0$ states and

$$\text{Prob} (cc \rightarrow T_{cc}[\bar{\mathbf{3}}, {}^3S_1]_{J=1}^{I=1}) \sim \begin{cases} \frac{1}{324} \eta_q^2, & J = 0 \\ \frac{1}{108} \eta_q^2, & J = 1 \\ \frac{5}{324} \eta_q^2, & J = 2 \end{cases} \quad (88)$$

$$\text{Prob} (cc \rightarrow T_{cc}[\mathbf{6}, {}^1S_0]_{J=1}^{I=1}) \sim \frac{1}{72} \eta_q^2, \quad (89)$$

for $I = 1$ states. Therefore, the ratio, $(T_{cc})/(\Xi_{cc})$, is given by

$$\frac{\text{Prob} (cc \rightarrow T_{cc}[\bar{\mathbf{3}}, {}^3S_1])}{\text{Prob} (cc \rightarrow \Xi_{cc})} \sim \frac{1}{4} \eta_q = 0.15 \sim 0.25, \quad (90)$$

$$\frac{\text{Prob} (cc \rightarrow T_{cc}[\mathbf{6}, {}^1S_0])}{\text{Prob} (cc \rightarrow \Xi_{cc})} \sim \frac{3}{8} \eta_q = 0.2 \sim 0.38. \quad (91)$$

Interestingly, we note that the ratio for productions of $T_{cc}[\bar{\mathbf{3}}, {}^3S_1]$ and $T_{cc}[\mathbf{6}, {}^1S_0]$ is independent of η_q ;

$$\frac{\text{Prob} (cc \rightarrow T_{cc}[\mathbf{6}, {}^1S_0])}{\text{Prob} (cc \rightarrow T_{cc}[\bar{\mathbf{3}}, {}^3S_1])} \sim 1.5. \quad (92)$$

Similarly, we obtain the relations between $I = 0$ and $I = 1$ productions as

$$\frac{\text{Prob}(\text{cc} \rightarrow \text{T}_{\text{cc}}[\bar{\mathbf{3}}, {}^3\text{S}_1])_{J=1}^{I=1}}{\text{Prob}(\text{cc} \rightarrow \text{T}_{\text{cc}}[\bar{\mathbf{3}}, {}^3\text{S}_1])} \sim \begin{cases} \frac{1}{3}, & J = 0 \\ 1, & J = 1 \\ \frac{5}{3}, & J = 2 \end{cases} \quad (93)$$

$$\frac{\text{Prob}(\text{cc} \rightarrow \text{T}_{\text{cc}}[\mathbf{6}, {}^1\text{S}_0])_{I=1}^{I=1}}{\text{Prob}(\text{cc} \rightarrow \text{T}_{\text{cc}}[\mathbf{6}, {}^1\text{S}_0])} \sim 1 \quad (94)$$

This simple model gives us a useful guidance on estimation of the production of T_{cc} accompanying light quark fragmentation.

5. Numerical results

5.1. Total cross sections

Now we present the numerical results of the total cross section. In the left panel of Fig. 4, we show the total cross sections σ_α of the T_{cc} production in the e^+e^- collisions with $m_c = 1.8$ GeV for both color configurations. The cross sections of the Ξ_{cc} production are plotted for comparison. We note that the mass of T_{cc} is $2m_c = 3.6$ GeV in the present framework, while the estimation by the constituent quark model is about 3.8 GeV. The strong coupling constant is chosen as $\alpha_s = 0.212$ at the scale $\mu_R = 2m_c$ [60], which was used for the production of Ξ_{cc} (see also Refs. [58, 59] for early works on Ξ_{cc}). We show the cross sections when the values of $R_{\text{cc}}(0)$ in set A in table 4 are used. The values of the cross sections in model B are about 1/4 of those in model A.

We find that the cross section of $\alpha = [\bar{\mathbf{3}}, {}^3\text{S}_1]$ is larger than that of $[\mathbf{6}, {}^1\text{S}_0]$. The difference is caused by the color-spin projection in Eqs. (67) and (68), as well as the probability factor in the light quark sector (86) and (87). In both cases, the cross sections start to increase at the threshold $2m_c$, as shown in the figures, and the peak of the production cross section is found around the energy slightly above the threshold ($\sqrt{s} \sim 10$ GeV). Near the Z boson pole ($\sqrt{s} \sim 90$ GeV), the cross section will be dominated by the contribution through the Z production over the γ^* production [60], but this is not included in the present discussion. For larger \sqrt{s} , the cross section decreases as being proportional to $1/s$.

To estimate the dependence on the quark mass, we also calculate the cross section with $m_c = 1.6$ GeV. The strong coupling constant is scaled by

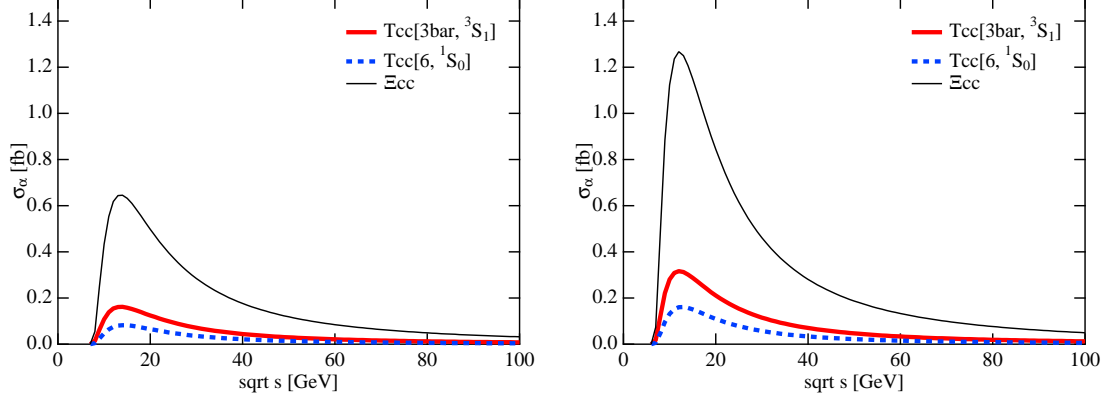


Figure 4: Total cross sections of the reaction $e^+e^- \rightarrow T_{cc}[\alpha] + X$ with $\alpha = [\bar{\mathbf{3}}, ^3S_1]$ (Thick solid lines) and $[\mathbf{6}, ^1S_0]$ (dashed lines). The thin solid lines represent the cross sections of the Ξ_{cc} production. The charm quark mass and the strong coupling constant are set to be $m_c = 1.8$ GeV and $\alpha_s = 0.212$ ($m_c = 1.6$ GeV and $\alpha_s = 0.221$) in the left (right) panel.

the two-loop running formula

$$\alpha_s(\mu_R) = \frac{1}{b_0 t} \left(1 - \frac{b_1 \ln t}{b_0 t} \right), \quad (95)$$

with $t = \ln(\mu_R^2/\Lambda^2)$, $b_0 = (33 - 2n_f)/12\pi$, $b_1 = (153 - 19n_f)/24\pi^2$ and $n_f = 3$. The nonperturbative scale $\Lambda = 0.239$ GeV is determined to reproduce $\alpha_s(3.6 \text{ GeV}) = 0.212$. This leads to $\alpha_s(3.2 \text{ GeV}) = 0.221$. In this case, the qualitative behavior of the cross section remains the same. The magnitude of the cross section increases by about factor two, mainly because of the increase of the phase space.

At the Belle energy $\sqrt{s} = 10.6$ GeV, total cross section is estimated as

$$\sigma_\alpha = \begin{cases} 0.0427 \text{ [fb]} & \text{for } \alpha = [\bar{\mathbf{3}}, ^3S_1]_{J=0}^{I=1} \\ 0.1281 \text{ [fb]} & \text{for } \alpha = [\bar{\mathbf{3}}, ^3S_1], [\bar{\mathbf{3}}, ^3S_1]_{J=1}^{I=1} \\ 0.2135 \text{ [fb]} & \text{for } \alpha = [\bar{\mathbf{3}}, ^3S_1]_{J=2}^{I=1} \\ 0.05762 \text{ [fb]} & \text{for } \alpha = [\mathbf{6}, ^1S_0], [\mathbf{6}, ^1S_0]^{I=1} \end{cases} \quad (96)$$

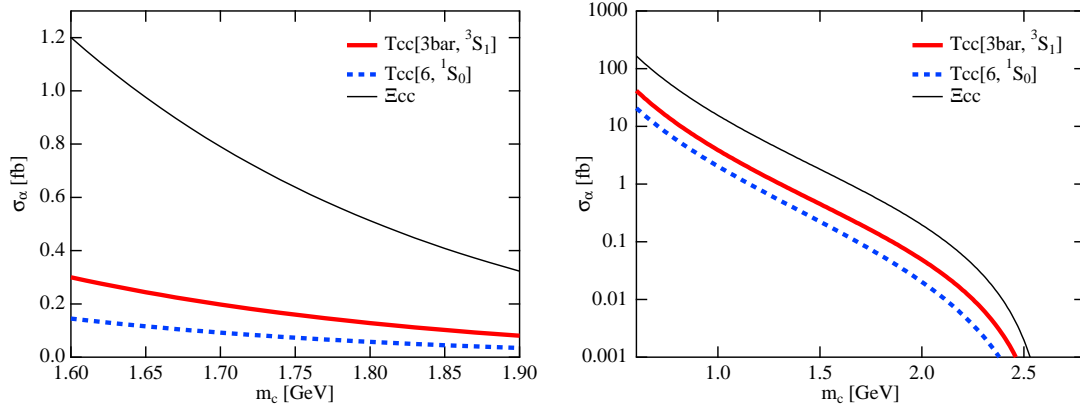


Figure 5: The quark mass dependence on the total cross sections of the reaction $e^+e^- \rightarrow T_{cc}[\alpha] + X$ with $\alpha = [\bar{\mathbf{3}}, {}^3S_1]$ (Thick solid lines) and $[\mathbf{6}, {}^1S_0]$ (dashed lines) at $\sqrt{s} = 10.6$ GeV. The thin solid lines represent the cross sections of the Ξ_{cc} production.

for $m_c = 1.8$ GeV and

$$\sigma_\alpha = \begin{cases} 0.1002 \text{ [fb]} & \text{for } \alpha = [\bar{\mathbf{3}}, {}^3S_1]_{J=0}^{I=1} \\ 0.3007 \text{ [fb]} & \text{for } \alpha = [\bar{\mathbf{3}}, {}^3S_1], [\bar{\mathbf{3}}, {}^3S_1]_{J=1}^{I=1} \\ 0.5012 \text{ [fb]} & \text{for } \alpha = [\bar{\mathbf{3}}, {}^3S_1]_{J=2}^{I=1} \\ 0.1451 \text{ [fb]} & \text{for } \alpha = [\mathbf{6}, {}^1S_0], [\mathbf{6}, {}^1S_0]_{J=1}^{I=1} \end{cases} \quad (97)$$

for $m_c = 1.6$ GeV. The quark mass dependence of the cross section around this region is shown in the left panel of Fig. 5 where the strong coupling constant is also scaled according to Eq. (95). We obtain the similar values for Ξ_{cc} in correspondence to $T_{cc}[\bar{\mathbf{3}}, {}^3S_1]$. Those values are comparable with the upper limit for the Ξ_{cc} cross section measured in Belle [85]. It may be interesting to compare the above numbers with the cross section of $e^+e^- \rightarrow J/\psi c \bar{c}$ estimated in the NRQCD framework at leading order, 0.27 pb [77].⁸ Our values given above for the $T_{cc} + \bar{c}c$ production are smaller than those for the $J/\psi c \bar{c}$ production, as expected.

A naive extrapolation of the present result in much wider range of the quark mass is shown in the right panel of Fig. 5. The threshold of the reaction is $\sqrt{s} = 4m_c$, so the cross section vanishes at $m_c = 2.65$ GeV. When

⁸At the next-to-leading order, the authors in Ref. [77] obtained 0.47 pb, which is comparable with 0.74 pb measured in Belle [57].

the quark mass is decreased, the cross section increases exponentially. At $m_c = 0.6$ GeV, the cross section is about a few pb order. This cross section, with multiplying the factor 1/4 to account for the electric charge of the quarks, formally corresponds to the Ξ production in the strangeness sector. Although this quark mass region is beyond the applicability of the NRQCD framework, we may regard it as a rough estimate of the Ξ production via the hard process. The dominant production mechanism of the strangeness at $\sqrt{s} = 10.6$ GeV is the color string breaking, so the contribution from the hard process should be smaller than the total cross section of the Ξ production. Nevertheless, it is interesting to observe that the present estimation may not be contradict with the experimental data measured by Belle, ~ 26 pb for Ξ production in e^+e^- collisions [86].

5.2. Differential cross sections

Next we show the differential cross section with respect to the momentum and angle of the final T_{cc} . To focus on the qualitative feature of the differential cross section, we calculate the normalized differential cross section defined as

$$\frac{1}{\sigma_\alpha} \frac{d\sigma_\alpha}{dp} = \frac{1}{\sigma_\alpha} \int d\cos\Theta \frac{d\sigma_\alpha}{dp d\cos\Theta}, \quad (98)$$

and

$$\frac{1}{\sigma_\alpha} \frac{d\sigma_\alpha}{d\cos\Theta} = \frac{1}{\sigma_\alpha} \int dp \frac{d\sigma_\alpha}{dp d\cos\Theta}. \quad (99)$$

These quantities are useful, because they are independent of the nonperturbative matrix element h_α . Hence the results in this subsection are independent of the choice of set A or B in table 4.

The results of the dependence on the momentum of T_{cc} at the Belle energy $\sqrt{s} = 10.6$ GeV, Eq. (98), are shown in Fig. 6 with $m_c = 1.8$ GeV and 1.6 GeV. Irrespective of the quark mass, we find the following qualitative difference depending on the color configurations. The peak position of $T_{cc}[\bar{\mathbf{3}}, {}^3S_1]$ is concentrated in the large p region. On the other hand, $T_{cc}[\mathbf{6}, {}^1S_0]$ is produced even with a small momentum $p \sim 1$ GeV where only a tiny fraction of $T_{cc}[\bar{\mathbf{3}}, {}^3S_1]$ can be produced.

Next we examine the dependence on Θ which is the production angle of T_{cc} measured from the collision axis. The results are shown in Fig. 7. The differential cross section has a symmetry under $\Theta \leftrightarrow \pi - \Theta$ because of the

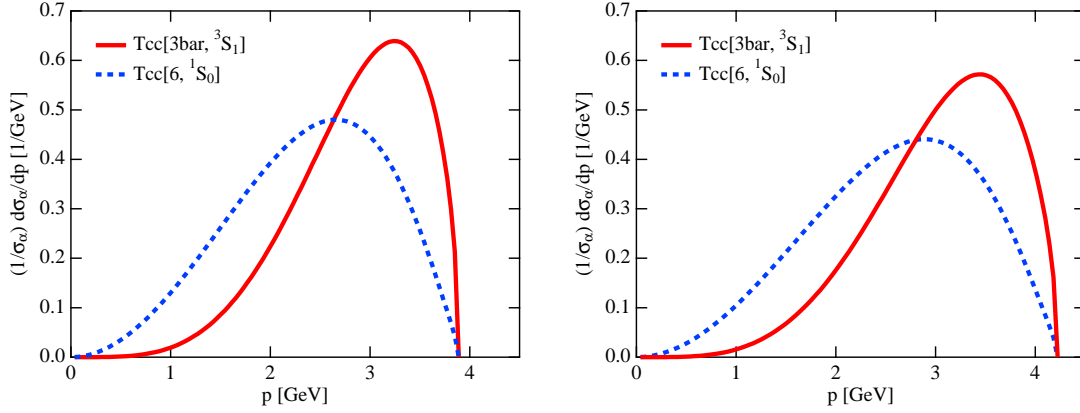


Figure 6: Momentum dependence of the normalized differential cross sections $(1/\sigma_\alpha)d\sigma_\alpha/dp$ of the reaction $e^+e^- \rightarrow T_{cc}[\alpha] + X$ with $\alpha = [\bar{\mathbf{3}}, {}^3S_1]$ (solid lines) and $[\mathbf{6}, {}^1S_0]$ (dashed lines) at $\sqrt{s} = 10.6$ GeV. The charm quark mass and the strong coupling constant are set to be $m_c = 1.8$ GeV and $\alpha_s = 0.212$ ($m_c = 1.6$ GeV and $\alpha_s = 0.221$) in the left (right) panel.

exchange of the electron and positron momenta. We find that $T_{cc}[\bar{\mathbf{3}}, {}^3S_1]$ is produced mainly in the transverse direction ($\Theta = \pi/2, 3\pi/2$), while the peak of the $T_{cc}[\mathbf{6}, {}^1S_0]$ is in the direction of the collision axis ($\Theta = 0, \pi$).⁹ Although the magnitude of the angular dependence is not strong, the $T_{cc}[\bar{\mathbf{3}}, {}^3S_1]$ production has opposite angular dependence from that of the $T_{cc}[\mathbf{6}, {}^1S_0]$.

In this way, we observe that the $T_{cc}[\alpha]$ states with different internal color configuration $[\alpha]$ provide qualitatively different momentum/angular dependence of the cross section. This will help the experimental distinction of the internal color configurations of $T_{cc}[\alpha]$.

6. Summary

We discuss the production of the doubly-charmed exotic hadron T_{cc} with quark content $cc\bar{u}\bar{d}$ from e^+e^- collisions. Based on the formalism of the NRQCD, we consider perturbative part of the productions of $cc\bar{c}\bar{c}$ via virtual

⁹If we decrease the quark mass further down to $\lesssim 1.4$ GeV, the peak of the $T_{cc}[\bar{\mathbf{3}}, {}^3S_1]$ production also lies in the direction of the collision axis. In this case, however, the mass of T_{cc} is lower than 2.8 GeV (the binding energy from the DD^* threshold is larger than 1 GeV). We consider such deep binding is unrealistic.

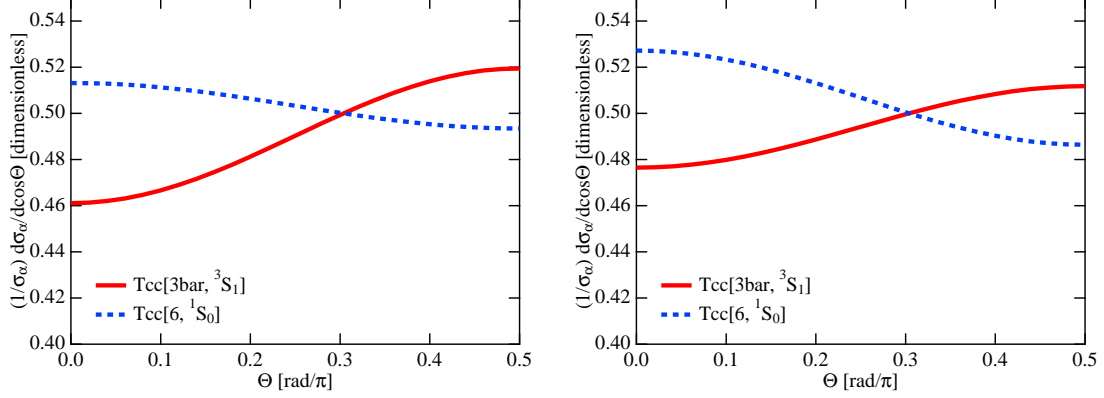


Figure 7: Angular dependence of the normalized differential cross sections $(1/\sigma_\alpha)d\sigma_\alpha/d\Theta$ of the reaction $e^+e^- \rightarrow T_{cc}[\alpha] + X$ with $\alpha = [\bar{\mathbf{3}}, {}^3S_1]$ (solid lines) and $[\mathbf{6}, {}^1S_0]$ (dashed lines) at $\sqrt{s} = 10.6$ GeV. The charm quark mass and the strong coupling constant are set to be $m_c = 1.8$ GeV and $\alpha_s = 0.212$ ($m_c = 1.6$ GeV and $\alpha_s = 0.221$) in the left (right) panel.

gamma from e^+e^- , and estimated the non-perturbative matrix elements from the non-relativistic quark model and the phenomenological estimation of the fragmentations of cc quark pair. The phenomenological discussion of the fragmentation, which was not considered in the previous work [62], induces a suppression for the cross sections by some factors. We also investigate the color structure of cc quark pairs with different color-spin structure, $T_{cc}[\bar{\mathbf{3}}, {}^3S_1]$ and $T_{cc}[\mathbf{6}, {}^1S_0]$. As a result, we estimate the cross sections of T_{cc} as 0.1281-0.3007 fb for $T_{cc}[\bar{\mathbf{3}}, {}^3S_1]$ and 0.05762-0.1451 fb for $T_{cc}[\mathbf{6}, {}^1S_0]$ depending on the parameter sets. It is also interesting to observe that the momentum- and angle-dependence of the cross sections of $T_{cc}[\bar{\mathbf{3}}, {}^3S_1]$ are qualitatively different from those of $T_{cc}[\mathbf{6}, {}^1S_0]$, and such information will be important to study the internal structure of T_{cc} in measurements in experiments.

Acknowledgments

S.Y. is supported by Grant-in-Aid for Scientific Research on Priority Areas “Elucidation of New Hadrons with a Variety of Flavors (E01: 21105006)”. This work was partly supported by the Grant-in-Aid for Scientific Research from MEXT and JSPS (Grant Nos. JP16K17694, JP25247036, JP15K17641 and JP17K05435) and by NNSFC (Grant No. 11275115).

References

- [1] Quarkonium Working Group, N. Brambilla et al., hep-ph/0412158.
- [2] E.S. Swanson, Phys. Rept. 429 (2006) 243.
- [3] M. Voloshin, Prog. Part. Nucl. Phys. 61 (2008) 455.
- [4] M. Nielsen, F.S. Navarra and S.H. Lee, Phys. Rept. 497 (2010) 41.
- [5] N. Brambilla et al., Eur. Phys. J. C 71 (2011) 1534.
- [6] A. Esposito, A. L. Guerrieri, F. Piccinini, A. Pilloni and A. D. Polosa, Int. J. Mod. Phys. A 30 (2015) 1530002.
- [7] H. X. Chen, W. Chen, X. Liu and S. L. Zhu, Phys. Rept. 639 (2016) 1.
- [8] A. Hosaka, T. Iijima, K. Miyabayashi, Y. Sakai and S. Yasui, PTEP 2016 (2016) 062C01.
- [9] R. F. Lebed, R. E. Mitchell and E. S. Swanson, Prog. Part. Nucl. Phys. 93 (2017) 143.
- [10] A. Ali, J. S. Lange and S. Stone, arXiv:1706.00610 [hep-ph].
- [11] Particle Data Group, C. Patrignani et al., Chin. Phys. C 40 (2016) no.10, 100001.
- [12] LEPS Collaboration, T. Nakano et al., Phys. Rev. Lett. 91 (2003) 012002.
- [13] LEPS Collaboration, T. Nakano et al., Phys. Rev. C 79 (2009) 025210.
- [14] Belle Collaboration, S. K. Choi et al., Phys. Rev. Lett. 100 (2008) 142001.
- [15] BESIII Collaboration, M. Ablikim et al., Phys. Rev. Lett. 110 (2013) 252001.
- [16] Belle Collaboration, A. Bondar et al., Phys. Rev. Lett. 108 (2012) 122001, 1110.2251.
- [17] LHCb Collaboration, R. Aaij et al., Phys. Rev. Lett. 115 (2015) 072001.

- [18] S. Zouzou et al., Z. Phys. C 30 (1986) 457.
- [19] H.J. Lipkin, Phys. Lett. B 172 (1986) 242.
- [20] J. Ader, J. Richard and P. Taxil, Phys. Rev. D 25 (1982) 2370.
- [21] L. Heller and J. Tjon, Phys. Rev. D 35 (1987) 969.
- [22] J. Carlson, L. Heller and J. Tjon, Phys. Rev. D 37 (1988) 744.
- [23] B. Silvestre-Brac and C. Semay, Z. Phys. C 57 (1993) 273.
- [24] B. Silvestre-Brac and C. Semay, Z. Phys. C 59 (1993) 457.
- [25] C. Semay and B. Silvestre-Brac, Z. Phys. C 61 (1994) 271.
- [26] S. Pepin et al., Phys. Lett. B 393 (1997) 119.
- [27] J. Schaffner-Bielich and A.P. Vischer, Phys. Rev. D 57 (1998) 4142.
- [28] D. Janc and M. Rosina, Few Body Syst. 35 (2004) 175.
- [29] M. Zhang, H. Zhang and Z. Zhang, Commun. Theor. Phys. 50 (2008) 437.
- [30] D. Brink and F. Stancu, Phys. Rev. D 57 (1998) 6778.
- [31] N. Barnea, J. Vijande and A. Valcarce, Phys. Rev. D 73 (2006) 054004.
- [32] J. Vijande, A. Valcarce and J.M. Richard, Phys. Rev. D 76 (2007) 114013.
- [33] J. Vijande et al., Phys. Rev. D 76 (2007) 094022.
- [34] J. Vijande et al., Phys. Rev. D 76 (2007) 094027.
- [35] J. Vijande, A. Valcarce and N. Barnea, Phys. Rev. D 79 (2009) 074010.
- [36] J. Vijande and A. Valcarce, Phys. Rev. C 80 (2009) 035204.
- [37] Y. Yang et al., Phys. Rev. D 80 (2009) 114023.
- [38] D. Ebert et al., Phys. Rev. D 76 (2007) 114015.
- [39] S.H. Lee et al., Eur. Phys. J. C 54 (2008) 259.

- [40] S.H. Lee and S. Yasui, Eur. Phys. J. C 64 (2009) 283.
- [41] A.V. Manohar and M.B. Wise, Nucl. Phys. B 399 (1993) 17.
- [42] N.A. Tornqvist, Z. Phys. C 61 (1994) 525.
- [43] G.J. Ding, J.F. Liu and M.L. Yan, Phys. Rev. D 79 (2009) 054005.
- [44] R. Molina, T. Branz and E. Oset, Phys. Rev. D 82 (2010) 014010.
- [45] S. Ohkoda et al., Phys. Rev. D 86 (2012) 014004.
- [46] T. Carames, A. Valcarce and J. Vijande, Phys. Lett. B 699 (2011) 291.
- [47] Y. Ikeda et al., Phys. Lett. B 729 (2014) 85.
- [48] T.D. Cohen and P.M. Hohler, Phys. Rev. D 74 (2006) 094003.
- [49] F.S. Navarra, M. Nielsen and S.H. Lee, Phys. Lett. B 649 (2007) 166.
- [50] M.L. Du et al., Phys. Rev. D 87 (2013) 014003.
- [51] ExHIC Collaboration, S. Cho et al., Phys. Rev. Lett. 106 (2011) 212001.
- [52] ExHIC Collaboration, S. Cho et al., Phys. Rev. C 84 (2011) 064910.
- [53] ExHIC Collaboration, S. Cho et al., Prog. Part. Nucl. Phys. 95 (2017) 279.
- [54] Belle Collaboration, K. Abe et al., Phys. Rev. Lett. 89 (2002) 142001.
- [55] Belle Collaboration, K. Abe et al., Phys. Rev. D 70 (2004) 071102.
- [56] BABAR Collaboration, B. Aubert et al., Phys. Rev. D 72 (2005) 031101.
- [57] Belle Collaboration, P. Pakhlov et al., Phys. Rev. D 79 (2009) 071101.
- [58] J. P. Ma and Z. G. Si, Phys. Lett. B 568 (2003) 135.
- [59] A. V. Berezhnoy and A. K. Likhoded, Phys. Atom. Nucl. 67 (2004) 757 [Yad. Fiz. 67 (2004) 778].
- [60] J. Jiang et al., Phys. Rev. D 86 (2012) 054021.
- [61] LHCb Collaboration, R. Aaij et al., arXiv:1707.01621 [hep-ex].

- [62] T. Hyodo, Y. R. Liu, M. Oka, K. Sudoh and S. Yasui, Phys. Lett. B 721 (2013) 56.
- [63] G.T. Bodwin, E. Braaten and G.P. Lepage, Phys. Rev. D 51 (1995) 1125.
- [64] A. Petrelli et al., Nucl. Phys. B 514 (1998) 245.
- [65] R.L. Jaffe, Phys. Rept. 409 (2005) 1.
- [66] D. B. Lichtenberg *et al.*, Phys. Rev. Lett. 48 (1982) 1653.
- [67] M.G. Alford, K. Rajagopal and F. Wilczek, Phys. Lett. B 422 (1998) 247.
- [68] R. Rapp et al., Phys. Rev. Lett. 81 (1998) 53.
- [69] M.G. Alford et al., Rev. Mod. Phys. 80 (2008) 1455.
- [70] S. Ohkoda et al., Phys. Rev. D 86 (2012) 034019.
- [71] S. Q. Luo, K. Chen, X. Liu, Y. R. Liu and S. L. Zhu, arXiv:1707.01180 [hep-ph].
- [72] T. Barnes, S. Godfrey and E. Swanson, Phys. Rev. D 72 (2005) 054026.
- [73] D. Flamm and F. Schoeberl, “Quantum numbers, gauge theories, and hadron spectroscopy” in “Introduction to the Quark Model of Elementary Particles” 1 (1982).
- [74] E. Braaten and J. Lee, Phys. Rev. D 67 (2003) 054007.
- [75] K.Y. Liu, Z.G. He and K.T. Chao, Phys. Lett. B 557 (2003) 45.
- [76] Y.J. Zhang, Y.j. Gao and K.T. Chao, Phys. Rev. Lett. 96 (2006) 092001.
- [77] Y. J. Zhang and K. T. Chao, Phys. Rev. Lett. 98 (2007) 092003.
- [78] G.T. Bodwin, J. Lee and C. Yu, Phys. Rev. D 77 (2008) 094018.
- [79] Y.J. Zhang, Y.Q. Ma and K.T. Chao, Phys. Rev. D 78 (2008) 054006.
- [80] DELPHI Collaboration, P. Abreu et al., Z. Phys. C 68 (1995) 375.

- [81] ALEPH Collaboration, R. Barate et al., Eur. Phys. J. C 2 (1998) 197.
- [82] CDF Collaboration, T. Affolder et al., Phys. Rev. Lett. 84 (2000) 1663.
- [83] CDF Collaboration, T. Aaltonen et al., Phys. Rev. D 77 (2008) 072003.
- [84] LHCb Collaboration, R. Aaij et al., Phys. Rev. D 85 (2012) 032008.
- [85] Belle Collaboration, Y. Kato et al., Phys. Rev. D 89 (2014) 052003.
- [86] Belle Collaboration, M. Sumihama, PoS Hadron 2013 (2013) 024.